(NASA-CR-161604) SHUTTLE SIMULATION TURBULENCE TAPES SSTT USERS GUIDE (Engineering Analysis, Inc.) 56 p HC A04/MF A01 CSCL 14B G3/14

N81-12134

Unclas 29369

NASA CONTRACTOR REPORT

NASA CR-161604

SHUTTLE SIMULATION TURBULENCE TAPES (SSTT) USERS GUIDE

By Frank B. Tatom and S. Ray Smith
Engineering Analysis, Inc.
2109 Clinton Avenue, Suite 432
Huntsville, Alabama 35805

September 1980

Prepared for

NASA - George C. Marshall Space Flight Center
Marshall Space Flight Center, Alabama 35812

TECHNICAL REPORT STANDARD TITLE PAGE

1. REPORT NO.	2. GOVERNMENT ACCESSION NO.	3. RECIPIENT'S CATALOG NO.
NASA CR-161604		
4. TITLE AND SUBTITLE Shuttle Simulation Turbulence Tapes (SSTT) Users Guide		5. REPORT DATE September 1980 6. PERFORMING ORGANIZATION CODE
7. AUTHOR(S) Frank B. Tatom and S. Ray Smith		8. PERFORMING ORGANIZATION REPORT # EAI-TR-80-002
9. PERFORMING ORGANIZATION NAME AND ADDRESS Engineering Analysis, Inc. 2109 Clinton Avenue, Suite 432 Huntsville, Alabama 35805		10. WORK UNIT NO. 11. CONTRACT OR GRANT NO. NAS8-33818 13. TYPE OF REPORT & PERIOD COVERED Contractor
12. SPONSORING AGENCY NAME AND ADDRESS National Aeronautics and Space Administration Washington, D.C. 20546		14. SPONSORING AGENCY CODE

15. SUPPLEMENTARY NOTES

Prepared under the technical monitorship of the Atmospheric Sciences Division, Space Sciences Laboratory, NASA/Marshall Space Flight Center, Alabama 35812

16. ABSTRACT

This document is a guide for potential users of Shuttle Simulation Turbulence Tapes (SSTT). It provides an appropriate description of the characteristics of the simulated turbulence stored on the tapes as well as instructions regarding their proper use. The characteristics of the turbulence series, including the spectral shape, cutoff frequencies, and variation of turbulence parameters with altitude, are discussed. Appendices present the results of spectral and statistical analyses of the SSTT.

17. KEY WORDS	18. DISTRIBUTION STATEMENT
	Unclassified—Unlimited Charles A. Lundquist Charles A. Lundquist Director, Space Sciences Laboratory

19. SECURITY CLASSIF. (of this report)	20. SECURITY CLASSIF. (of this page)	21. NO. OF PAGES	22. PRICE
Unclassified	Unclassified	53	NTIS

MSFC - Form 3292 (Rev. December 1972)

For sale by National Technical Information Service, Springfield, Virginia 22151

TABLE OF CONTENTS

LIST OF TABLES

LIST OF TABLES
(Continued)

LIST OF ILLUSTRATIONS

LIST OF ILLUSTRATIONS
(Continued)

LIST OF ILLUSTRATIONS
(Continued)

1. INTRODUCTION

The effects of atmospheric turbulence in both horizontal and near-horizontal flight, during the return of the Space Shuttle, are important for determining design, control, and "pilot-in-the-loop" effects. A non-recursive model (based on von Karman spectra) for atmospheric turbulence along the flight path of the Shuttle Orbiter has been developed which provides for simulation of instantaneous vertical and horizontal gusts at the vehicle center-of-gravity, and also for simulation of instantaneous gust gradients. Based on this model the time series for both gusts and gust gradients have been generated and stored on a series of magnetic tapes which are entitled Snuttle Simulation Turbulence Tapes (SSTT). The time series are designed to represent atmospheric turbulence from ground level to an altitude of 10,000 meters.

The purpose of this document is to provide any potential user of the SSTT with an appropriate description of the characteristics of the simulated turbulence stored on the tapes, as well as instructions regarding their proper use. Section 2 contains a discussion of the characteristics of the turbulence series, including the spectral shape, cutoff frequencies, and variation of turbulence parameters with altitude. Information regarding the tapes and their use is presented in Section 3. References cited are included in Section 4. Appendices A and B present the results of spectral and statistical analyses of the SSTT.

2. CHARACTERISTICS OF SIMULATED TURBULENCE

The non-recursive turbulence model used to generate the SSTT is based on von Karman spectra with finite upper limits corresponding to the dimensions of the Space Shuttle, relative to the scale of turbulence in the atmosphere. Because the scale of turbulence increases with altitude while the dimensions of the Space Shuttle are fixed, the finite upper limits of the von Karman spectra increase with altitude. In order to take into account these spectral changes, for each gust or gust gradient there are actually four time series corresponding to four altitude bands extending from ground level to 10,000 meters, as indicated in Table 2-1. A more detailed description of the characteristics of the turbulence is provided in the subsections which follow.

TABLE 2-1. TURBULENCE PARAMETERS FOR ALTITUDE BANDS

Band #	Lower Limit (m)	Upper Limit (m)	Time Interval (dimensionless)	Finite Limit of Spectrum (dimensionless)			Von Karman Length Scale (m)		
			T	Ω_{1MAX}	Ω_{2MAX}	Ω_{3MAX}	L_1	L_2	L_3
1	0	30	.6018	5.22	3.38	7.22	47	30	18
2	30	100	.2300	13.66	11.14	31.27	123	99	78
3	100	762	.09431	33.31	33.76	120.27	300	300	300
4	762	10000	.05309	59.18	59.97	213.68	533	533	533

2.1 TURBULENCE GENERATION PROCEDURE

The six types of SSTT are presented in Table 2-2. For each gust and gust gradient series indicated in the table, the generation procedure involved convolving a discrete white noise signal of unit variance with a discrete approximation of the impulse response function corresponding to the appropriate, dimensionless spectrum [1]. Each of the resulting series consists of 8500 discrete signals. The time interval associated with each series was based on the maximum frequency for which the simulation procedure is considered valid.

TABLE 2-2. TYPES OF SIMULATED TURBULENCE

Type	Corresponding Spectrum	Comments
u_1	Φ_{11}	longitudinal gust
u_2	Φ_{22}	transverse gust
u_3	Φ_{33}	vertical gust
$\partial u_2/\partial x_1$	$\Phi_{22/11}$	yaw
$\partial u_3/\partial x_1$	$\Phi_{33/11}$	pitch
$\partial u_3/\partial x_2$	$\Phi_{33/22}$	roll

These time intervals and the corresponding limiting frequencies, Ω_{IMAX}, are included in Table 2-1. The limiting frequencies were calculated according to the relation

$$\Omega_{imax} = aL_i/\ell_i \tag{2-1}$$

where

a = 1.30
L_i = scale of the i-th component of atmospheric turbulence
ℓ_i = characteristic length of Space Shuttle in i-th direction

Values of L_i for the four bands are given in Table 2-1 while the characteristic lengths, ℓ_i, are presented in Table 2-3. It is important to note that the values of L_i correspond to von Karman spectra as opposed to Dryden spectra and were derived from the local isotropy requirement discussed in subsection 3.2.

TABLE 2-3. CHARACTERISTIC DIMENSIONS OF THE SPACE SHUTTLE

Characteristic Length	Magnitude (ft)	(m)	Explanation
ℓ_1	39.56*	12.06*	mean aerodynamic chord
ℓ_2	39.05	11.9	1/2 wingspan
ℓ_3	10.95	3.34	1/2 fuselage thickness

2.2 DIMENSIONLESS ENERGY CONTENT

The total dimensionless energy content of each time series for each altitude band was established by integrating the corresponding spectra over the appropriate finite limits indicated in Table 2-1. The resulting energy content is presented in Table 2-4. As might be expected the total dimensionless energy content of each of the turbulent gust series is less than unity. The

TABLE 2-4. DIMENSIONLESS ENERGY CONTENT FOR GUSTS AND GUST GRADIENTS

Spectrum	Altitude Band			
	1	2	3	4
Φ_{11}	.5388	.7841	.8956	.9298
Φ_{22}	.5772	.7942	.8952	.9296
Φ_{33}	.5225	.7646	.8809	.9197
$\Phi_{22/11}$	1.2832	6.6484	24.768	54.125
$\Phi_{33/11}$	1.1321	5.9699	22.644	49.528
$\Phi_{33/22}$	.7049	4.9954	22.893	50.057

*This value is slightly greater than that previously reported [1] and is derived from a more accurate source [2].

dimensionless energy* content for each gust gradient, however, is not limited in such a manner and range as high as 54.125. For both gusts and gust gradients the total energy content increases with altitude because of similar increases in the limits of integration.

2.3 VALIDATION OF SIMULATED TURBULENCE

A spectral analysis of each of the dimensionless time series has been carried out by means of a Fast Fourier Transform FFT4 [3]. The results, which are presented in Appendix A, demonstrate that the simulated turbulence possesses the proper von Karman spectral characteristics.

All of the dimensionless time series have also been analyzed statistically to determine the gust and gust gradient probability density functions. As shown in Appendix B the results of these analyses indicate that both the simulated gusts and gust gradients are normally distributed, with near-zero means and standard deviations consistent with the energy content presented in Table 2-4.

*Actually the term "energy" is not precise when dealing with gust gradients.

3. USE OF SIMULATED TURBULENCE TAPES

The dimensionless simulated turbulence time series are stored on six magnetic tapes as summarized in Table 3-1. Each tape actually contains four time series corresponding to the four altitude bands described in Section 2. The appropriate procedures for reading the tapes are presented in subsection 3.1, while the proper method for converting the time series from dimensionless to dimensional form is described in subsection 3.2.

TABLE 3-1. INDEX OF SHUTTLE SIMULATED TURBULENCE TAPES (SSTT)

Tape	Time Series	Comments
SSTT-1	u_1 - gust	longitudinal gust
SSTT-2	u_2 - gust	transverse gust
SSTT-3	u_3 - gust	vertical gust
SSTT-4	$\partial u_2/\partial x_1$ - gust gradient	yaw
SSTT-5	$\partial u_3/\partial x_1$ - gust gradient	pitch
SSTT-6	$\partial u_3/\partial x_2$ - gust gradient	roll

3.1 READING THE TIME SERIES TAPES

The four time series on each tape are stored in parallel in 4-word logical records and are correlated (i.e., at any point in the time series the 4 turbulence values are all generated from the same string of random numbers). Each time series consists of 8500 elements and thus each tape contains 8500 4-word records. Pertinent characteristics of the tapes are summarized in Table 3-2.

The first record on each tape contains a 36-character alphanumeric descriptor. The second record contains the time series identification number (1-6), the number of points in the time series, and the dimensionless generation time step size for each altitude band. The format for this record is

TABLE 3-2 MAGNETIC TAPE CHARACTERISTICS

Number of tracks:	9
Header type:	Non-label
Character type:	7-bit ASCII
Recording density:	800 bits per inch

"2I10,4(1X,E14.7)". Following these two records, the time series is stored in 4-word records as previously described and in the format "4(1X,E14.7)". The order of storage in each record is from lowest to highest altitude band. Thus the first word in each record corresponds to band #1, the second to band #2, etc.

In the actual use of the time series tapes the sampling frequency may be different from the frequency at which the tapes were generated. In fact, the dimensionless sampling frequency will generally be variable. Therefore it will be necessary to interpolate the time series in order to get values at the proper points in dimensional time. Either zero-order or first-order interpolation should be used. Also, as time progresses and altitude changes, it will be necessary to switch altitude bands in the time series consistent with Table 2-1. Because of the manner in which the 4 time series are generated, any discontinuity due to switching time series should be minimal.

3.2 CONVERSION TO DIMENSIONAL VALUES

The dimensionless time series on each tape must be converted to dimensional form before actual use in a simulation exercise. The conversion process generally involves multiplication and/or division by the appropriate turbulence parameters. For dimensionless gusts, u_i, the corresponding standard deviation, σ_i, should be used. Thus

$$u_i^* = \sigma_i u_i \qquad (3\text{-}1)$$

where

u_i^* = dimensional gust

For dimensionless gust gradient, $\frac{\partial u_i}{\partial x_j}$, the parameters σ_i and L_j are used. Thus

$$\frac{\partial u_i^*}{\partial x_j^*} = \frac{\sigma_i}{L_j}\frac{\partial u_i}{\partial x_j} \tag{3-2}$$

where

$\partial u_i^* / \partial x_j^*$ = dimensional gust gradient

Conversion of dimensionless time step, T, involves vehicle velocity, V, and the x-component of turbulence scale, L_1. Thus

$$\Delta t^* = aL_1T/V \tag{3-3}$$

where

Δt^* = dimensional time step

It is important to note that because both L_1 and V vary with altitude, the dimensional time step Δt^* is not a constant. To obtain dimensional time, t^*, a summation process is involved as follows:

$$\begin{aligned} t_N^* &= \sum_{n=0}^{N} \Delta t_n^* \\ &= aT\sum_{n=0}^{N} L_{1n}/V_n \end{aligned} \tag{3-4}$$

where

L_{1n} = $L_1(Z_n)$

V_n = $V(Z_n)$

Z_n = altitude at nth step

The variation of the turbulence standard deviation, σ_i, with altitude is presented in Table 3-3. The same table contains the turbulence scale, L_i, as a function of altitude. Notice should be taken that the values for σ_i and L_i presented are designed for use with von Karman spectral models and therefore differ somewhat from previously tabulated values [4] which were designed for use with Dryden spectra. The von Karman σ_i and L_i have been computed based on the requirement for local isotropy, which can be expressed as

$$\frac{\sigma_1^2}{L_1^{2/3}} = \frac{\sigma_2^2}{L_2^{2/3}} = \frac{\sigma_3^2}{L_3^{2/3}} \qquad (3\text{-}5)$$

This method of computation is consistent with the established procedure [5].

The vehicle speed, V, is a function of altitude but also may vary from one trajectory to another. Table 3-4 provides representative values of V as a function of altitude.

TABLE 3-3. VARIATION OF VON KARMAN STANDARD DEVIATION AND LENGTH SCALE WITH ALTITUDE

ALTITUDE (m)	STANDARD DEVIATION OF TURBULENCE			INTEGRAL SCALES OF TURBULENCE		
	σ_1(m/sec)	σ_2(m/sec)	σ_3(m/sec)	L_1(m)	L_2(m)	L_3(m)
10	1.79	1.49	1.12	19	10	5
20	2.15	1.80	1.48	34	20	11
30	2.39	2.06	1.74	47	30	18
40	2.57	2.26	1.95	59	40	26
50	2.73	2.43	2.14	70	50	34
60	2.86	2.58	2.30	82	60	42
70	2.98	2.72	2.44	92	70	51
80	3.09	2.84	2.58	103	80	60
90	3.19	2.95	2.70	113	89	69
100	3.28	3.05	2.81	123	99	78
200	3.93	3.83	3.71	214	197	180
300	4.37	4.37	4.36	296	295	294
304.8						
400						
500	4.39	4.39	4.39	300	300	300
600						
700						
762						
800	5.7	5.7	5.7			
900						
1524						
2000	5.79	5.79	5.79			
3048						
4000	5.52	5.52	5.52	533	533	533
5000						
6096						
7000	5.27	5.27	5.27			
8000						
9144						
10000	4.22	4.22	4.22			

TABLE 3-4. VARIATION OF SHUTTLE VELOCITY WITH ALTITUDE [6]

ALTITUDE (m)	V (m/sec)
100	152
300	156
500	158
2000	170
4000	188
6000	200
8000	240
10000	300

4. REFERENCES CITED

1. Tatom, Frank B., and Smith, S. Ray, "Atmospheric Turbulence Simulation for Shuttle Orbiter", *EAI-TR-79-[illegible]*, Engineering Analysis, Inc., Huntsville, Alabama, August 31, 1979.

2. Rockewell International Corporation, "Aerodynamic Design Substantiation Report", *SD74-SH-[illegible]*, 1974.

3. Maynard, Harry W., "An Evaluation of Ten Fast Fourier Transform (FFT) Programs", *Research and Development Technical Report ECOM-5476*, U.S. Army Electronics Command, Fort Monmouth, NJ, March 1973.

4. Space Shuttle Program: Natural Environment Design Requirements. Appendix 10.10, Space Shuttle Flight and Ground Specification, Level II Program Definition and Requirements, *[illegible]*, vol. X, Revision B. NASA-Lyndon B. Johnson Space Center, Houston, TX, August 18, 1975.

5. Chalk, C. R., et al, "Background Information and User Guide for MIL-F-8785B(ASG), 'Military Specification - Flying Qualities of Piloted Airplanes'", Air Force Flight Dynamics Laboratory, Air Force Systems Command, Wright-Patterson Air Force Base, Ohio, *AFFDL-TR-69-72*, August 1969.

6. Fichtl, George H., "A Technique for Simulating Turbulence for Aerospace Vehicle Flight Simulation Studies", *NASA TM [illegible]*, George C. Marshall Space Flight Center, Marshall Space Flight Center, AL, November 1977.

APPENDIX A

SPECTRAL ANALYSIS OF SIMULATED TURBULENCE

By means of a Fast Fourier Transform [3] spectral analyses of all simulated turbulence have been performed. The results are presented in dimensionless form in Figures A-1 through A-24. Table A-1 provides a summary of these figures. Also included in each figure is the theoretical von Karman spectra. The agreement between the theoretical spectra and the computed spectra is quite satisfactory.

TABLE A-1. MATRIX OF SPECTRAL ANALYSIS FIGURES

SERIES TYPE	ALTITUDE BAND			
	1	2	3	4
u_1	A-1	A-2	A-3	A-4
u_2	A-5	A-6	A-7	A-8
u_3	A-9	A-10	A-11	A-12
$\partial u_2/\partial x_1$	A-13	A-14	A-15	A-16
$\partial u_3/\partial x_1$	A-17	A-18	A-19	A-20
$\partial u_3/\partial x_2$	A-21	A-22	A-23	A-24

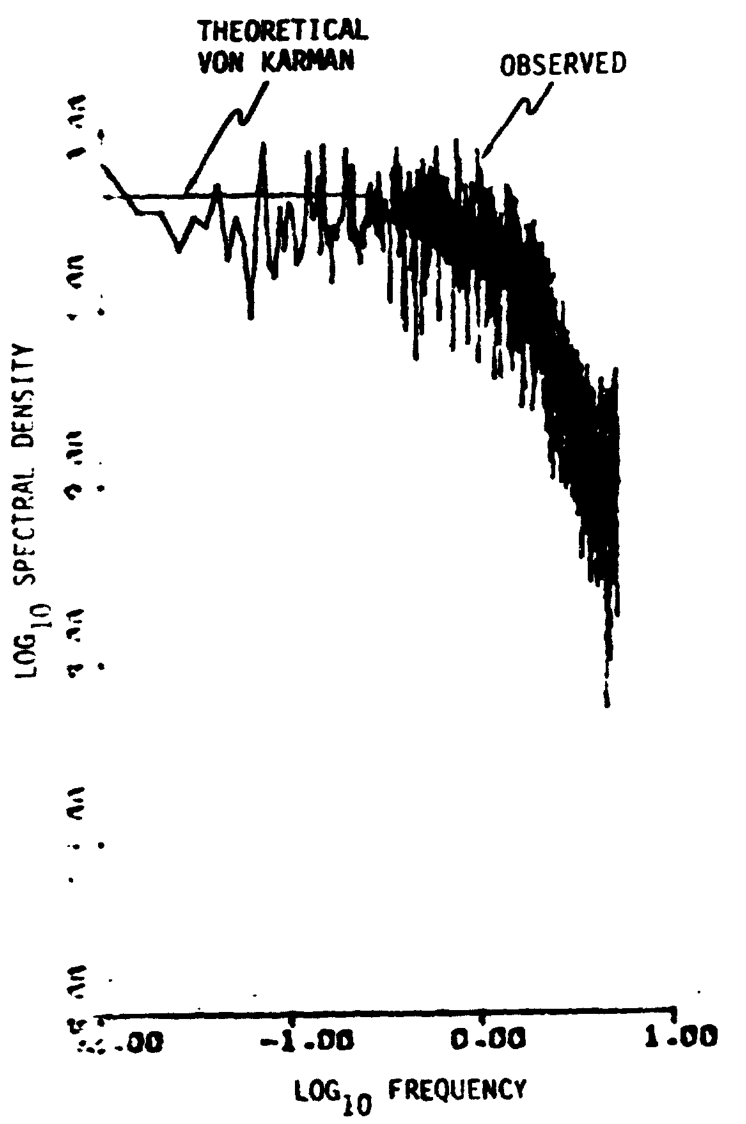

Figure A-1. u_1 - Gust Spectrum, Altitude Band #1

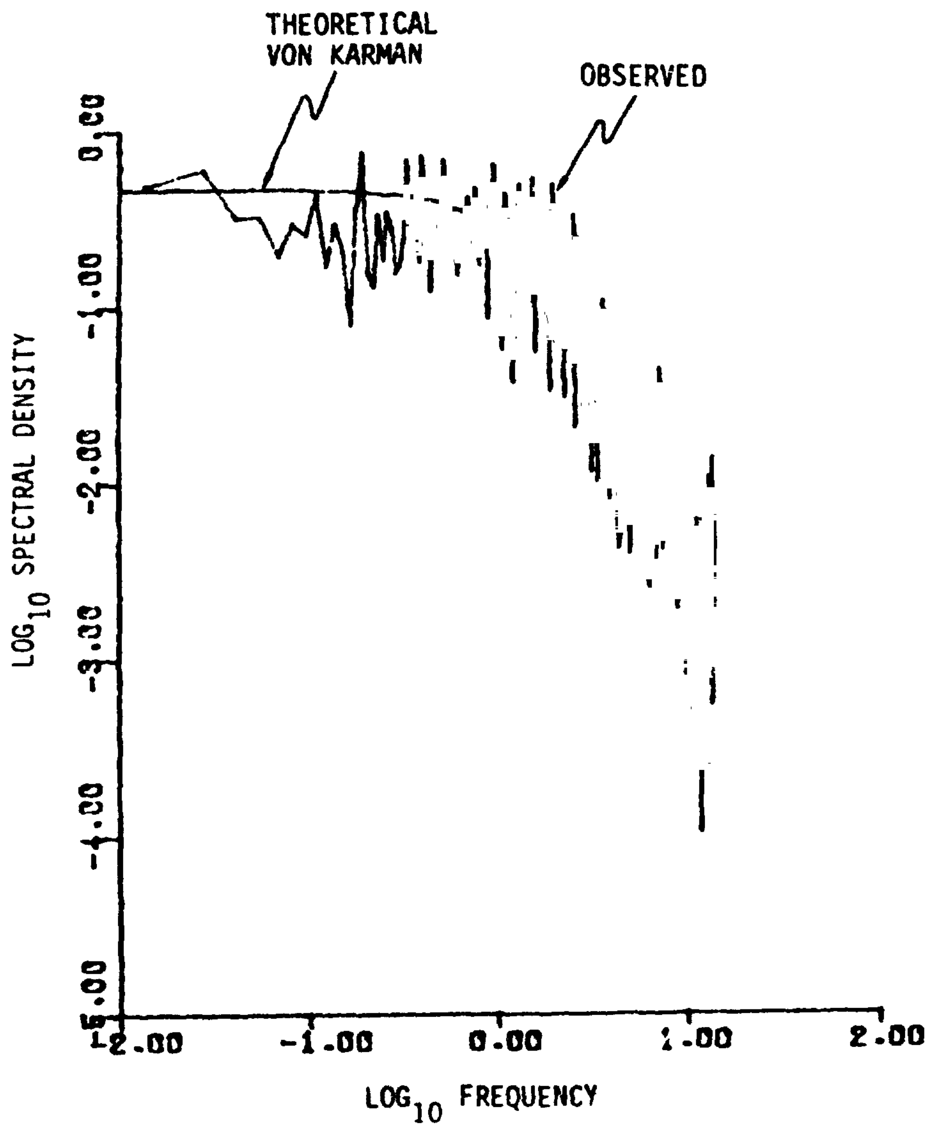

Figure A-2. u_1 - Gust Spectrum, Altitude Band #2

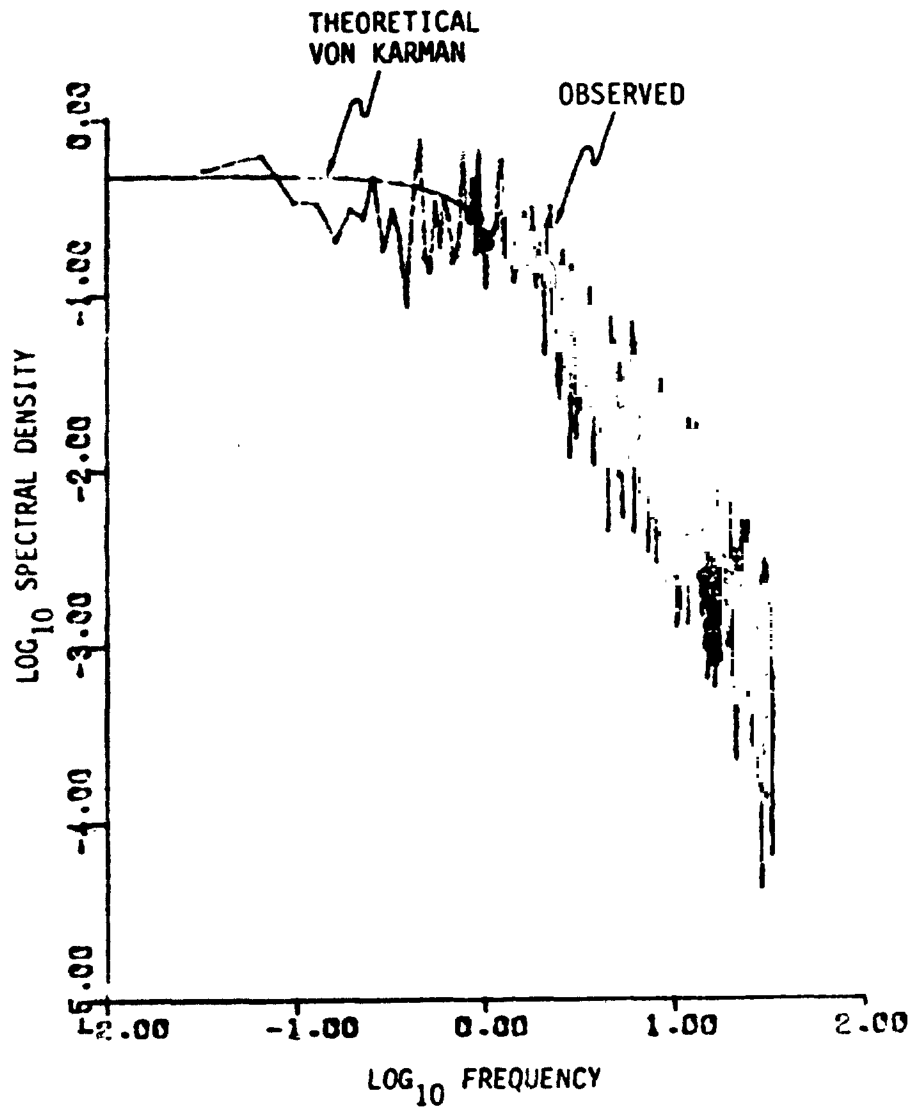

Figure A-3. u_1 - Gust Spectrum, Altitude Band #3

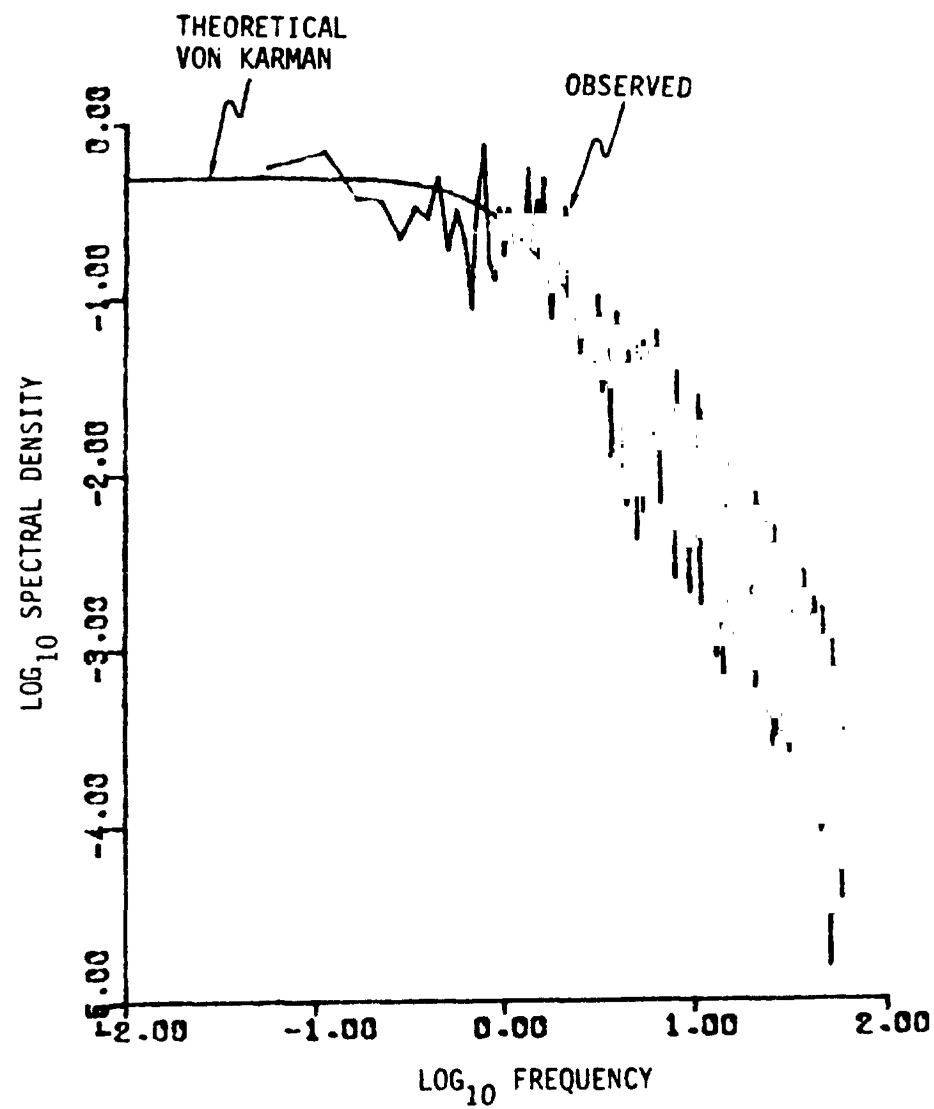

Figure A-4. u_1 - Gust Spectrum, Altitude Band #4

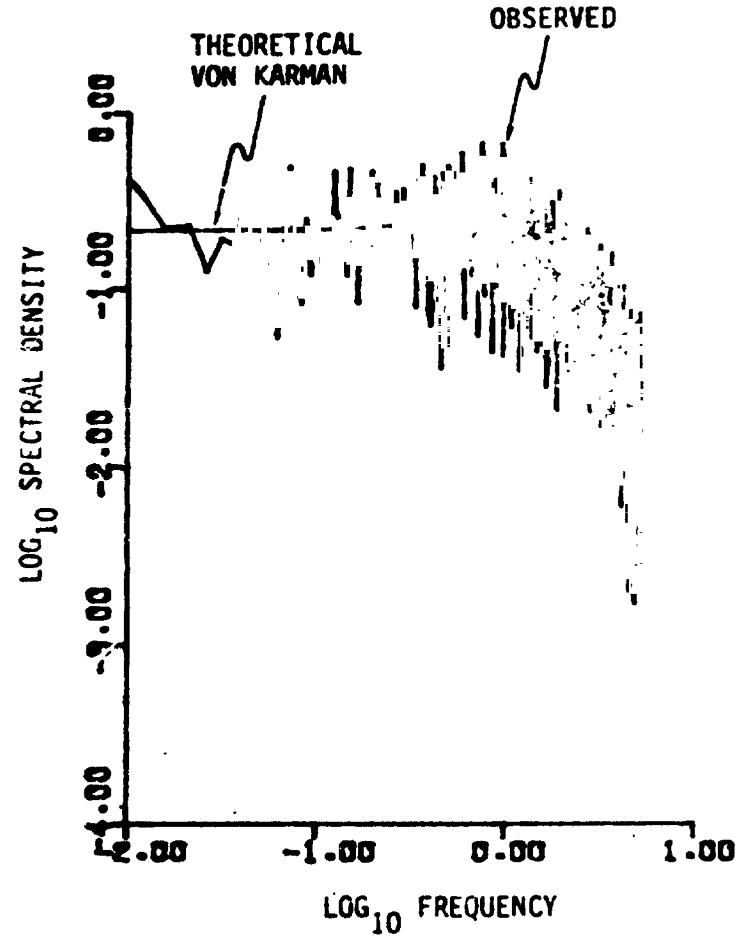

Figure A-5. u_2 - Gust Spectrum, Altitude Band #1

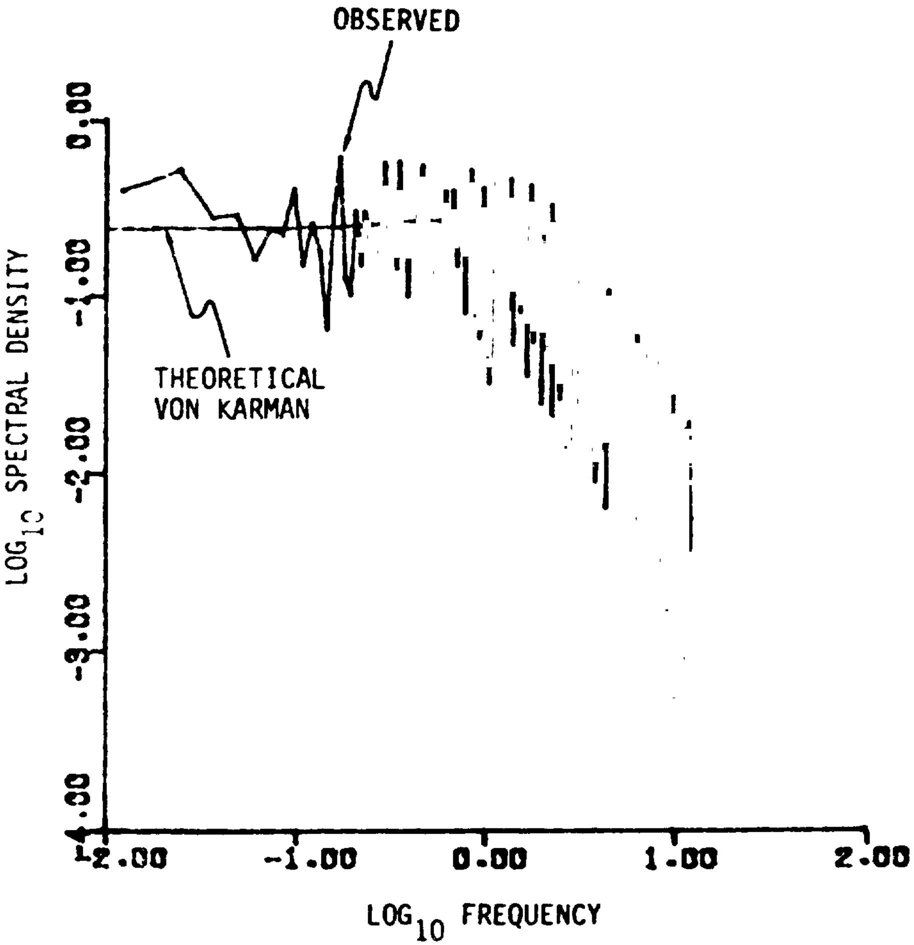

Figure A-6. u_2 - Gust Spectrum, Altitude Band #2

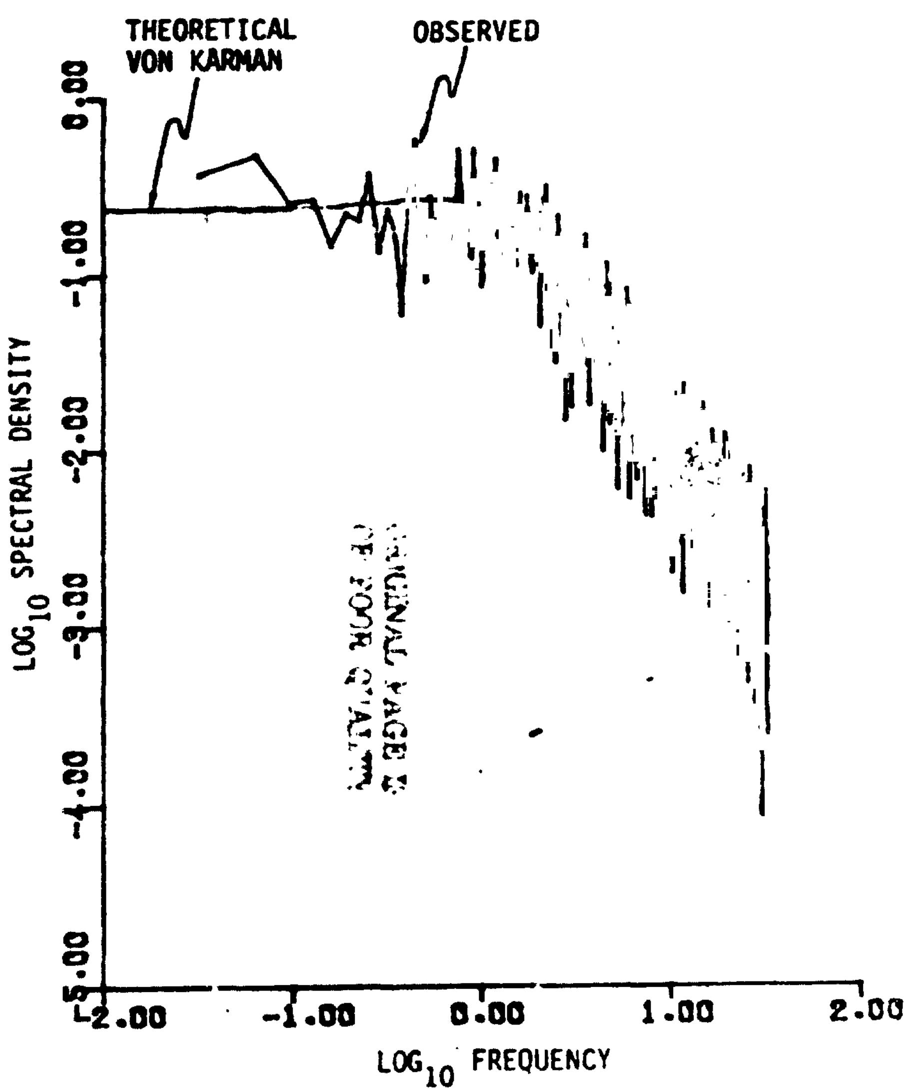

Figure A-7. u_2 - Gust Spectrum, Altitude Band #3

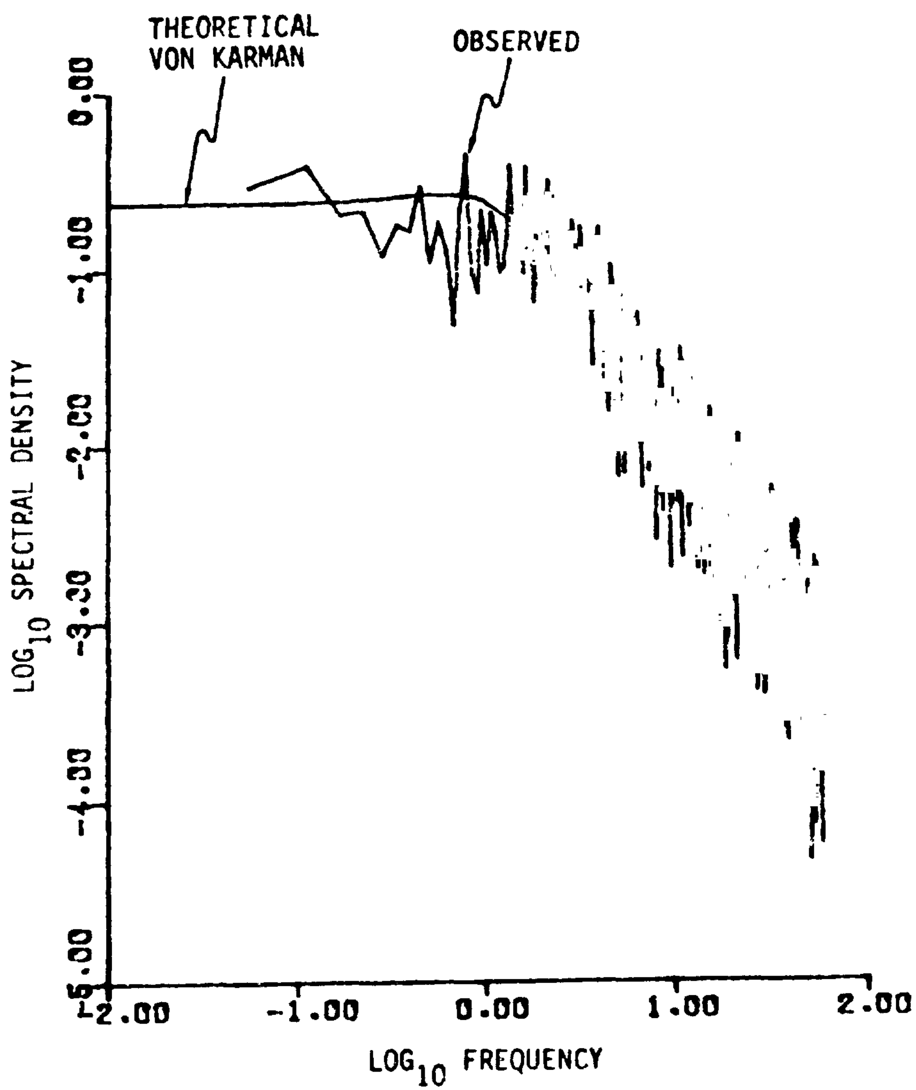

Figure A-8. u_2 - Gust Spectrum, Altitude Band #4

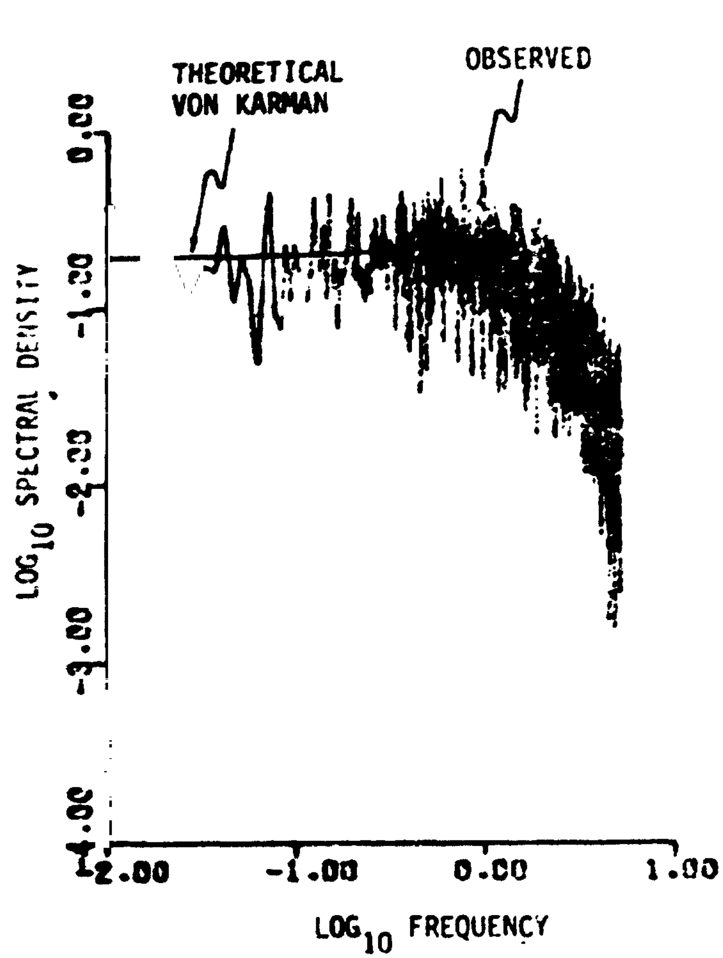

Figure A-9. u_3 - Gust Spectrum, Altitude Band #1

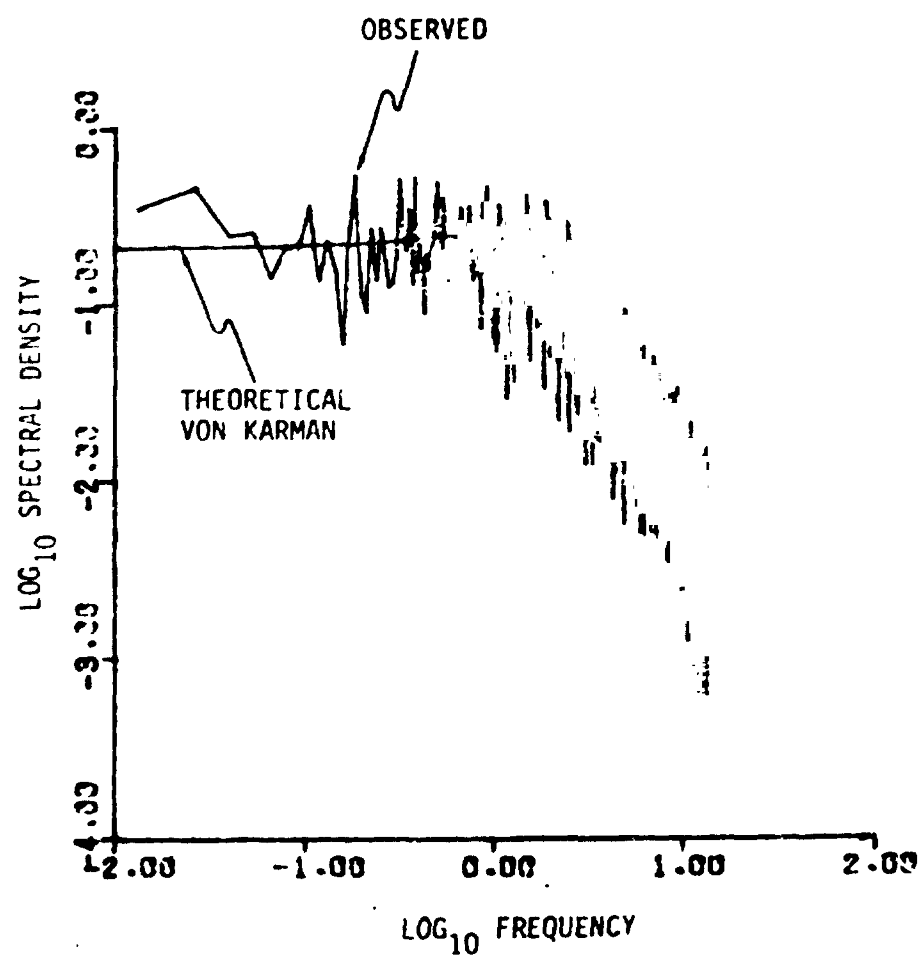

Figure A-10. u_3 - Gust Spectrum, Altitude Band #2

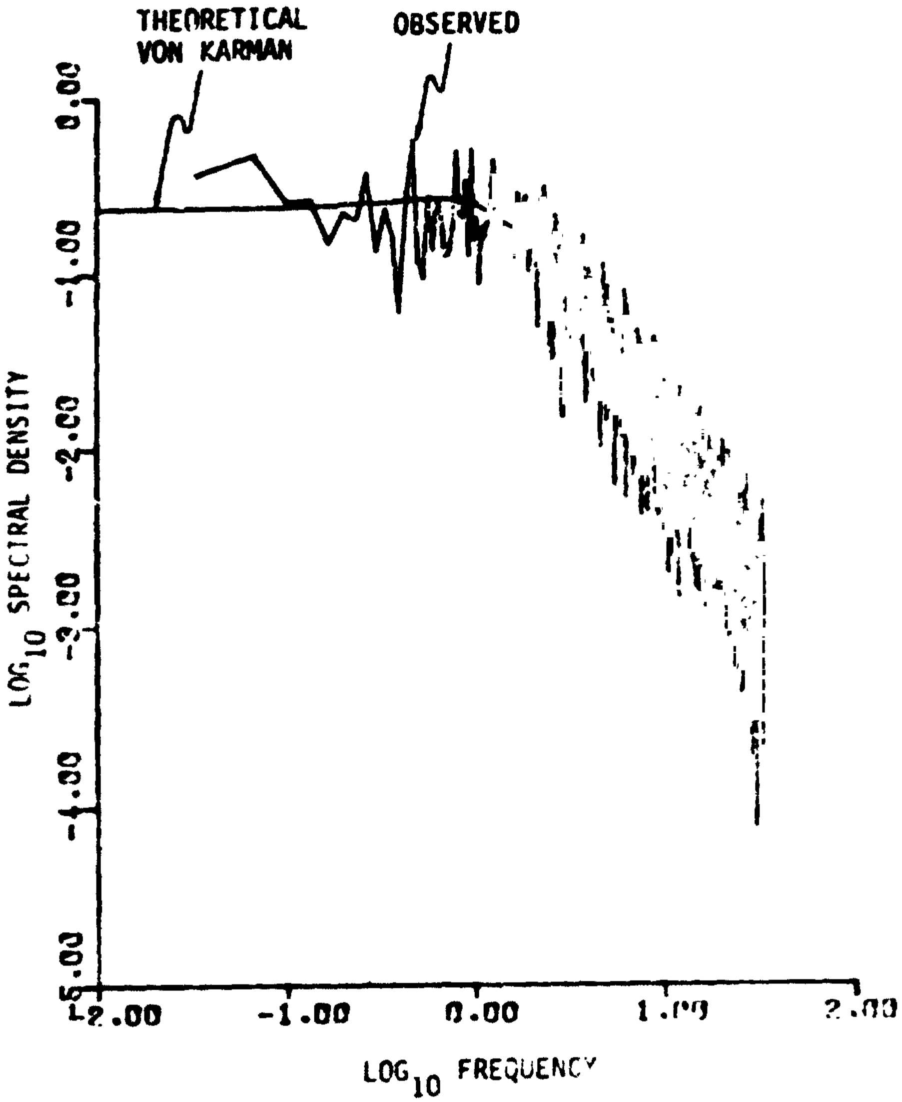

Figure A-11. u_3 - Gust Spectrum, Altitude Band #3

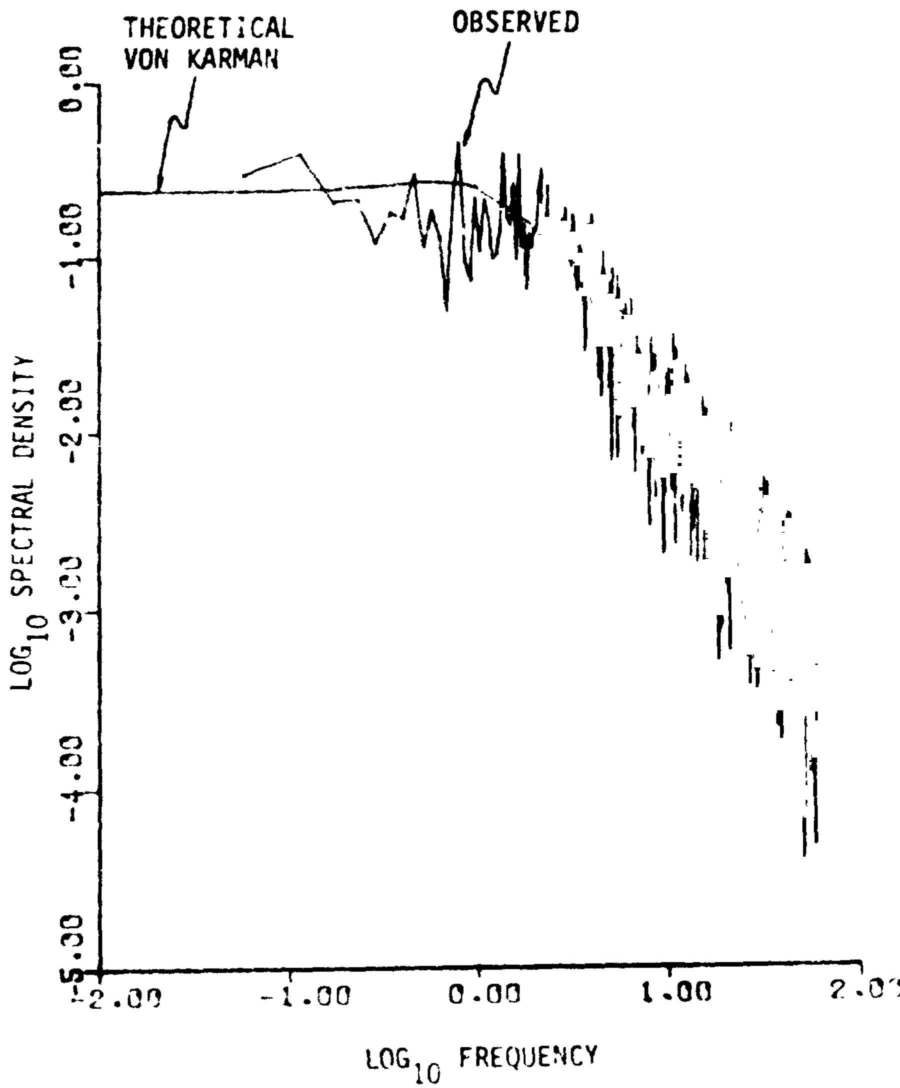

Figure A-12. u_3 - Gust Spectrum, Altitude Band #4

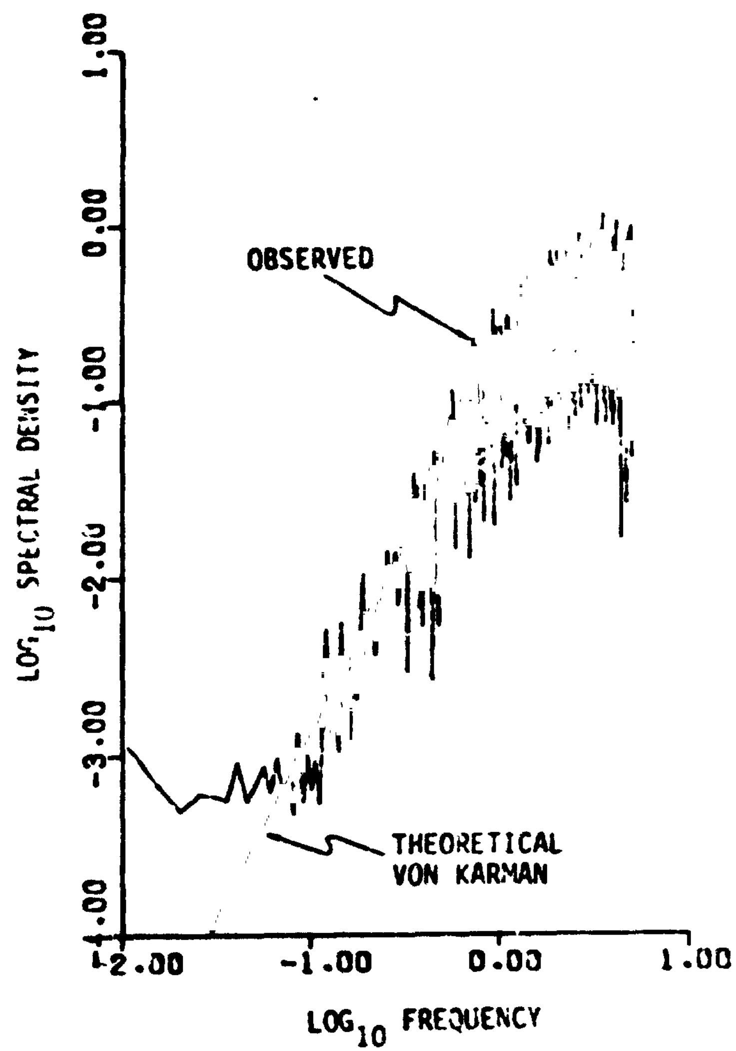

Figure A-13. $\partial u_2/\partial x_1$ - Gust Gradient Spectrum, Altitude Band #1

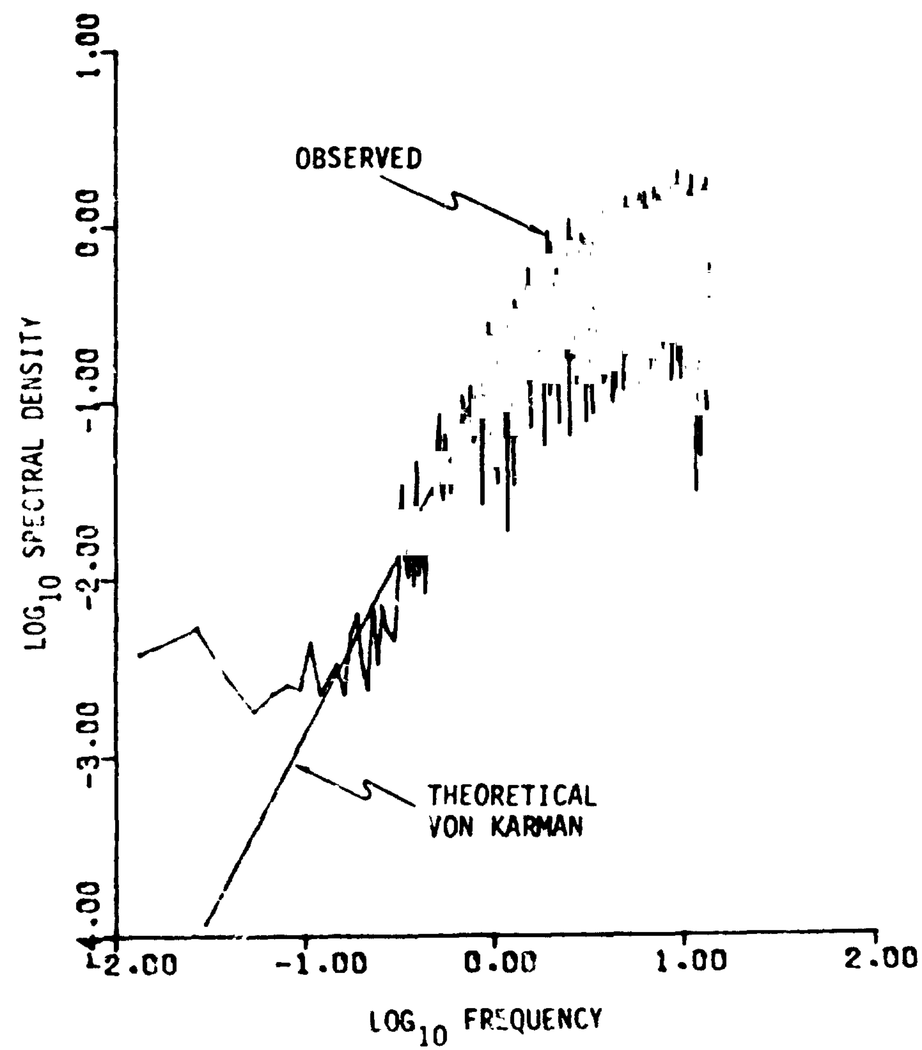

Figure A-14. $\partial u_2/\partial x_1$ - Gust Gradient Spectrum, Altitude Band #2

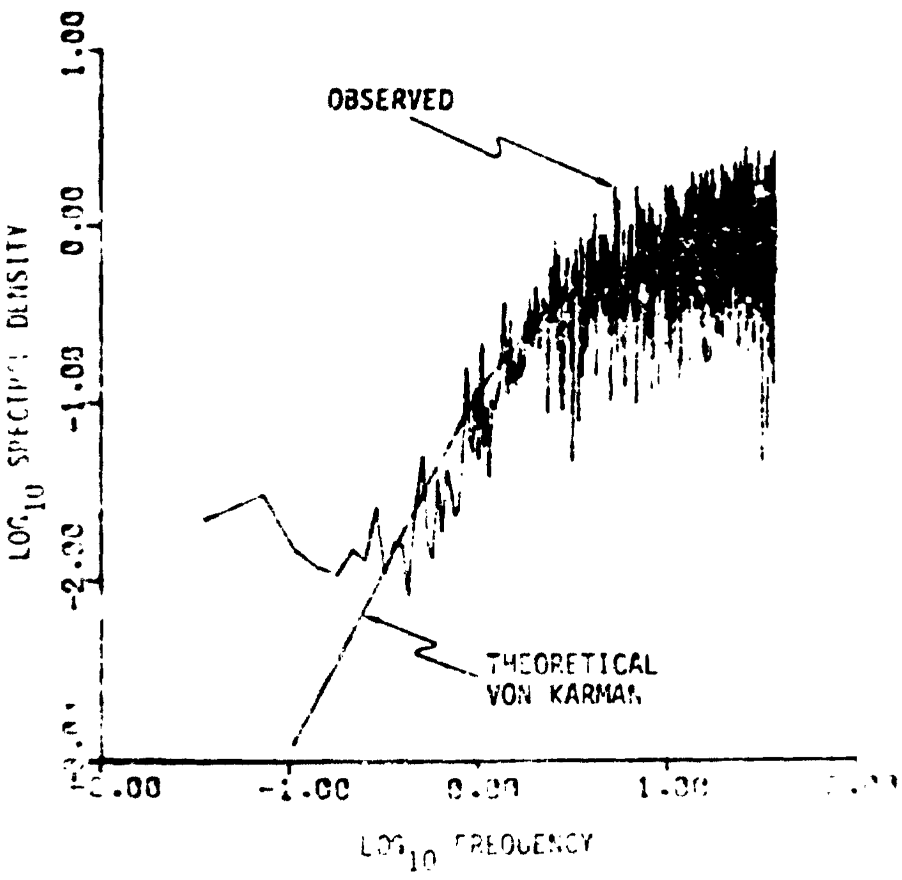

Figure A-15. $\partial u_2/\partial x_1$ - Gust Gradient Spectrum, Altitude Band #3

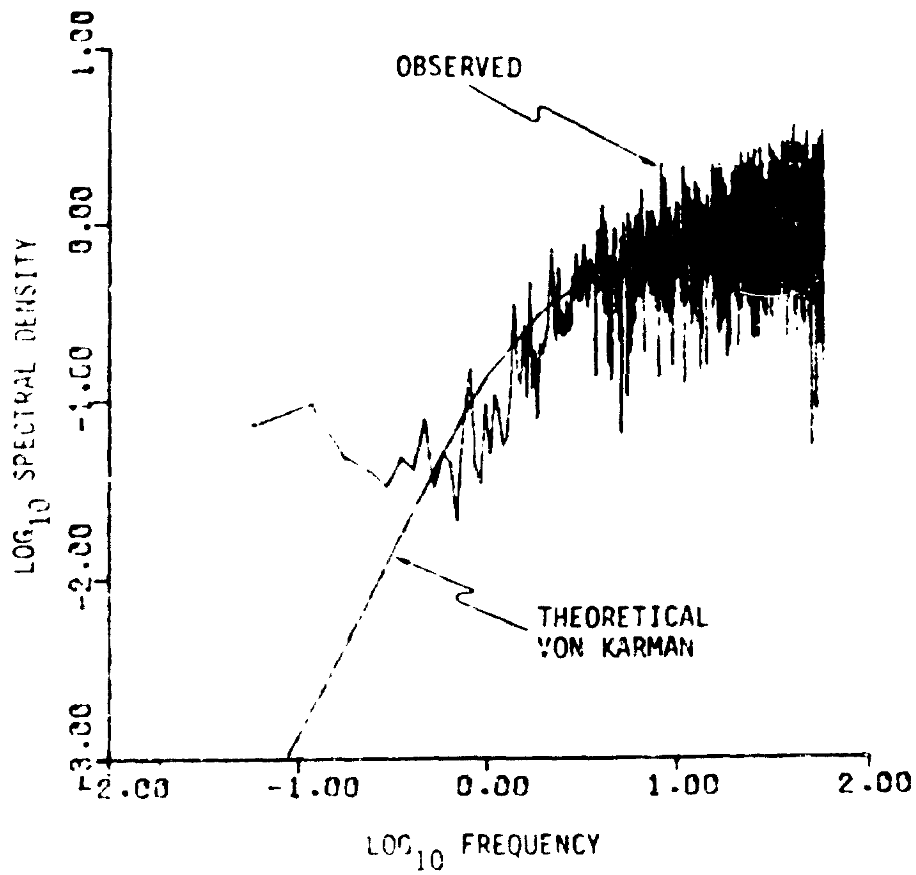

Figure A-16. $\partial u_2/\partial x_1$ - Gust Gradient Spectrum, Altitude Band #4

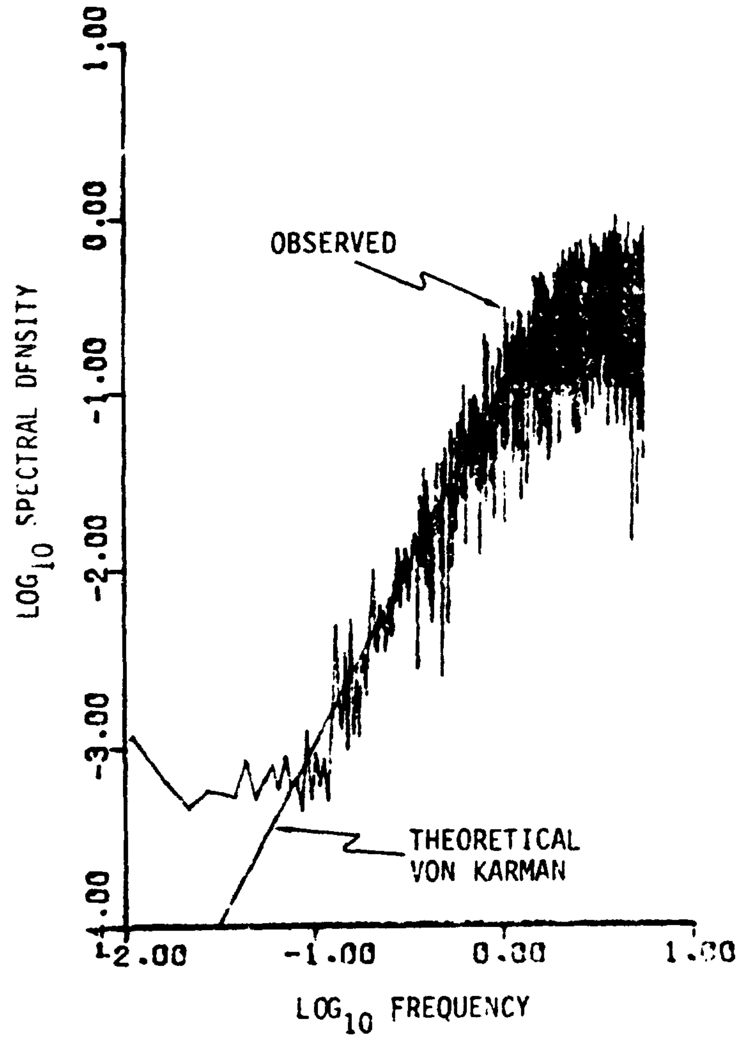

Figure A-17. $\partial u_3/\partial x_1$ - Gust Gradient Spectrum, Altitude Band #1

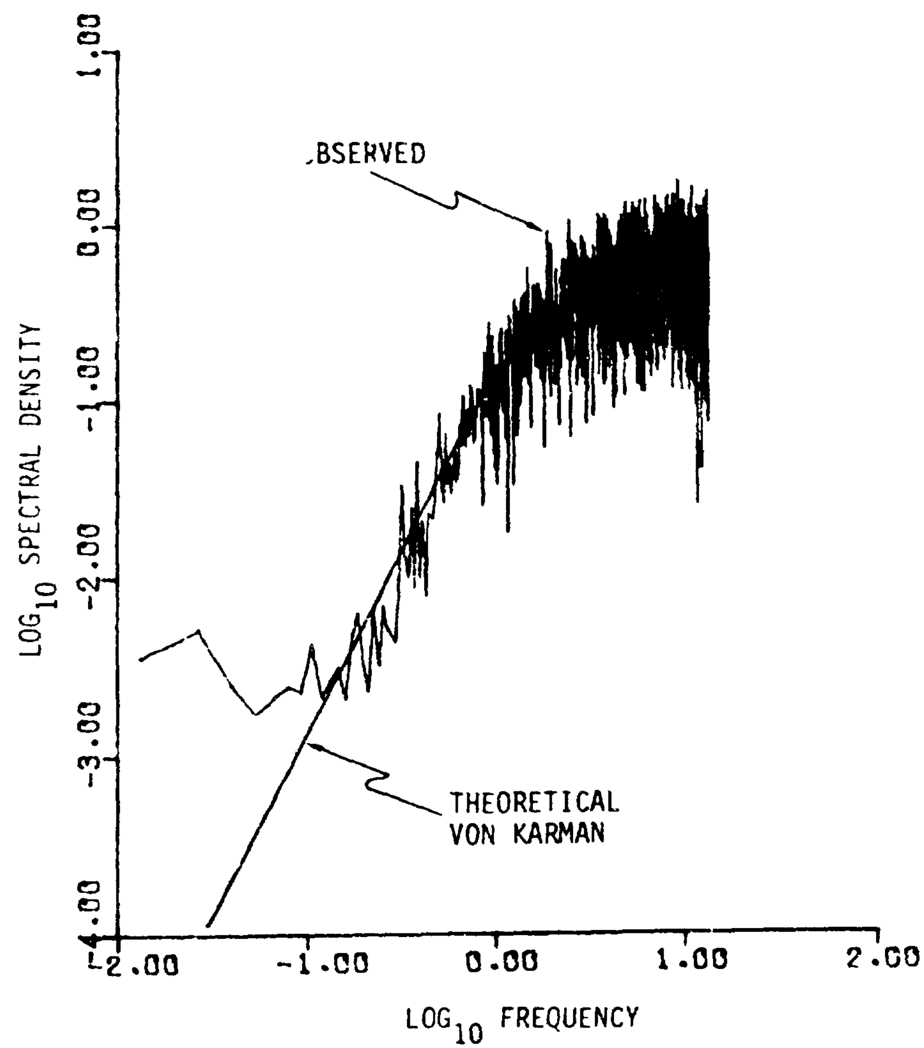

Figure A-18. $\partial u_3/\partial x_1$ - Gust Gradient Spectrum, Altitude Band #2

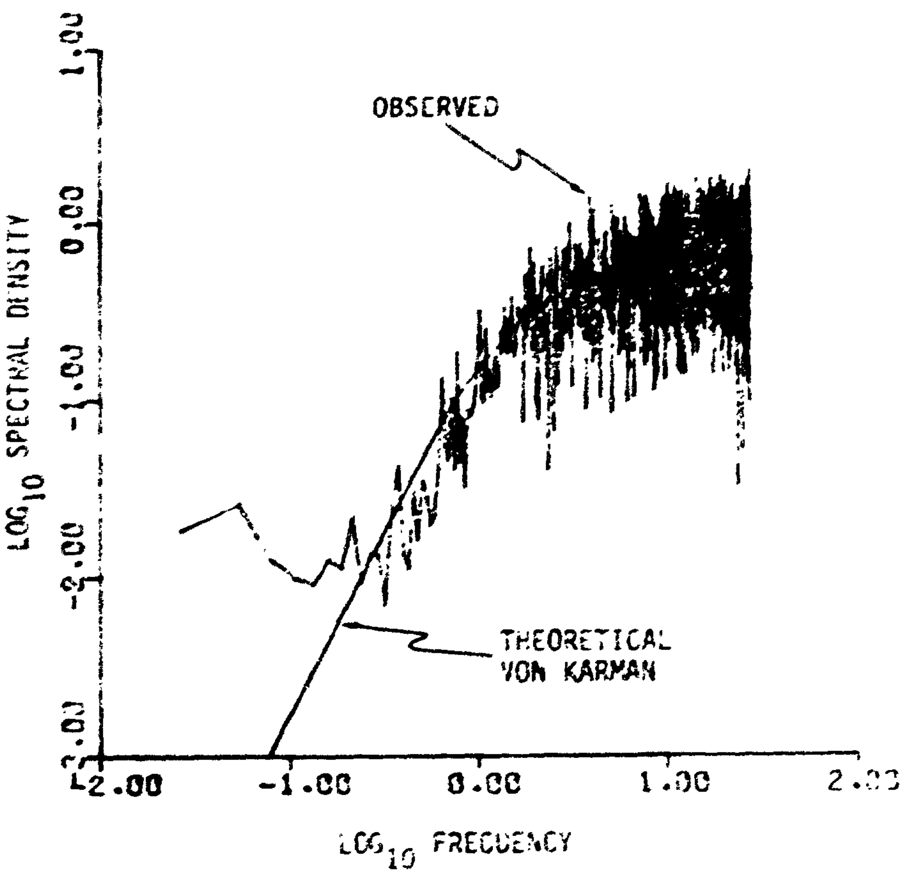

Figure A-19. $\partial u_3/\partial x_1$ - Gust Gradient Spectrum, Altitude Band #3

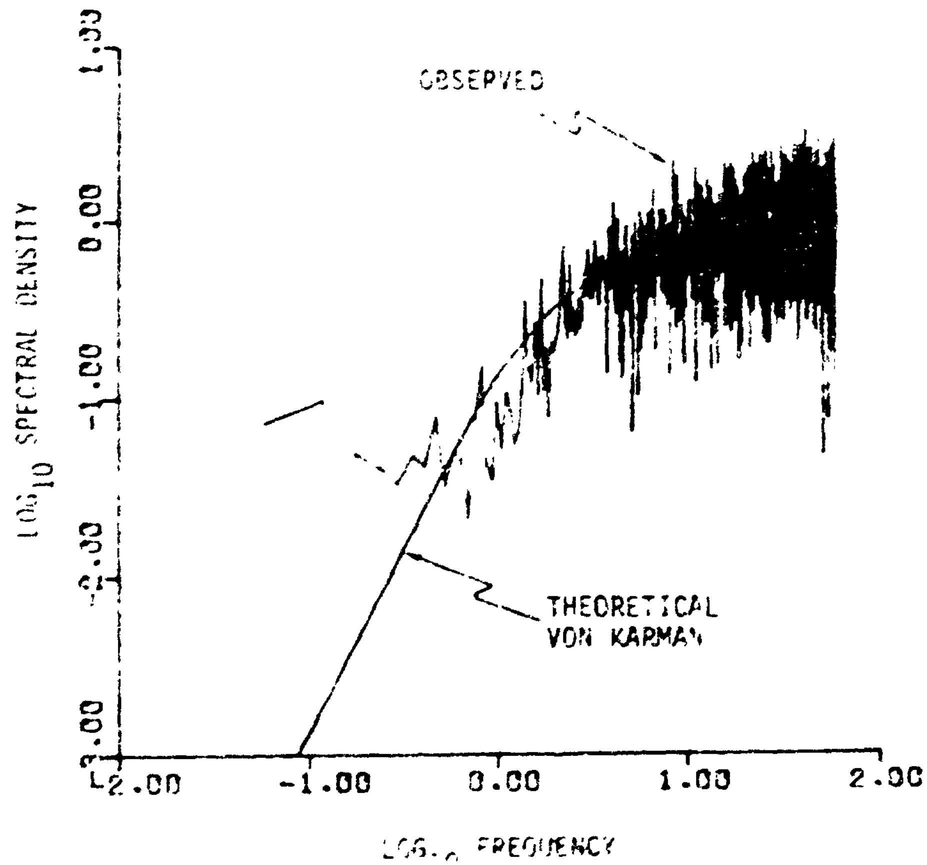

Figure A-20. $\partial u_3/\partial x_1$ - Gust Gradient Spectrum, Altitude Band #4

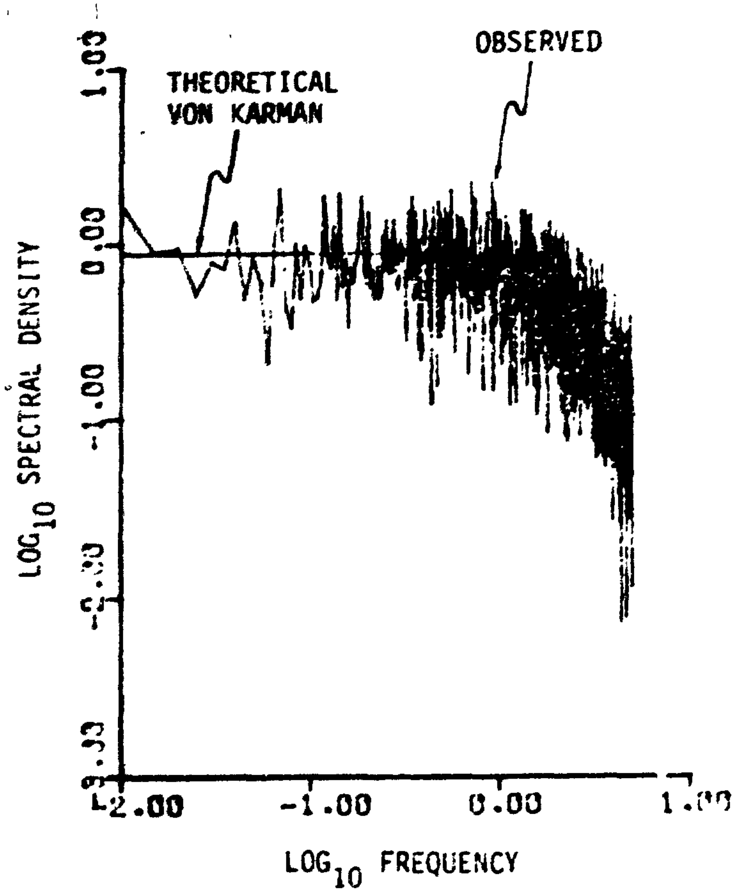

Figure A-21. $\partial u_3/\partial x_2$ - Gust Gradient Spectrum, Altitude Band #1

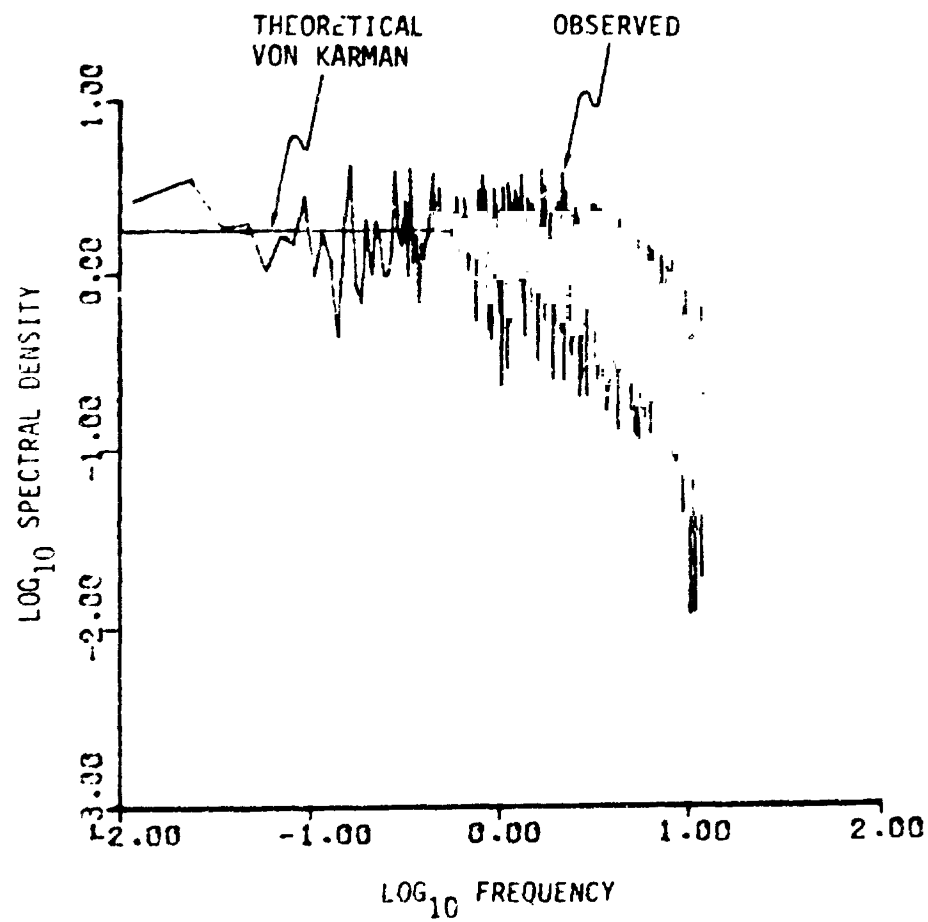

Figure A-22. $\partial u_3/\partial x_2$ - Gust Gradient Spectrum, Altitude Band #2

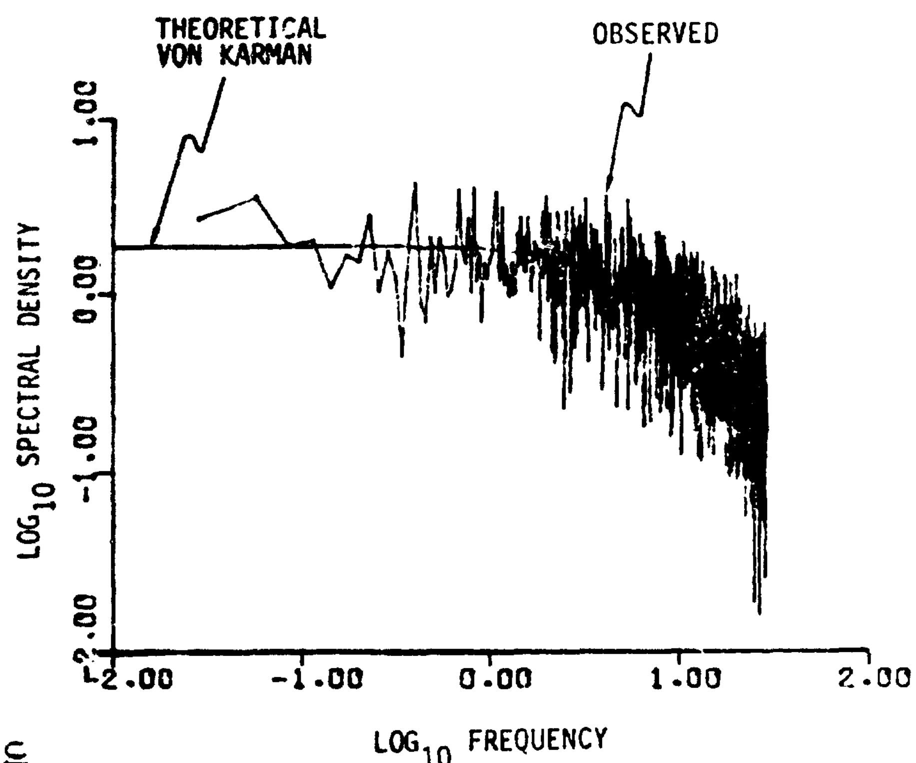

Figure A-23. $\partial u_3/\partial x_2$ - Gust Gradient Spectrum, Altitude Band #3

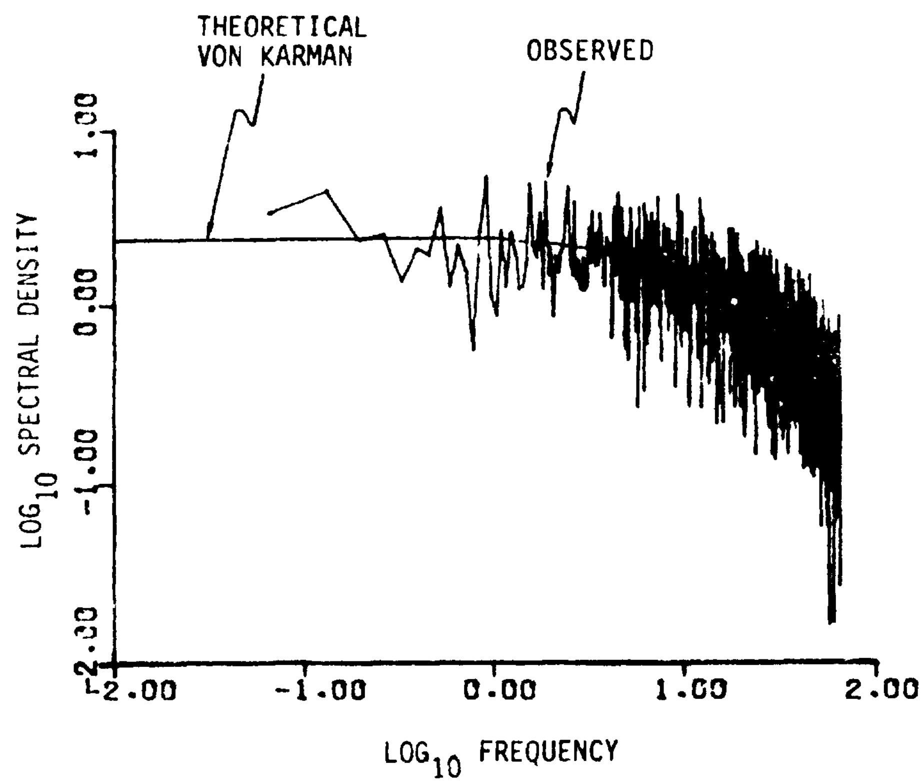

Figure A-24. $\partial u_3/\partial x_2$ - Gust Gradient Spectrum, Altitude Band #4

ORIGINAL PAGE IS
OF POOR QUALITY

APPENDIX B

STATISTICAL ANALYSIS OF SIMULATED TURBULENCE

By means of standard statistical analysis procedures each of the SSTT has been analyzed to determine its mean value, standard deviation, and probability density distribution. The resulting mean values are presented in Table B-1 while Table B-2 contains the resulting standard deviations. As expected all mean values were near zero. The standard deviations represent the square root of the energy content. The ratio of the square root of each theoretical energy content (from Table 2-4) to the corresponding standard deviation (from Table B-2) is presented in Table B-3. The agreement appears quite satisfactory.

The gust and gust gradient probability density distributions are presented in Figures B-1 through B-24 in accordance with Table B-4. In each figure the corresponding normal distribution is also presented. The results indicate that both the gust and gust gradient time series are very close to normal distributions.

TABLE B-1. MEAN VALUE OF GUST AND GUST GRADIENTS

SERIES TYPE	ALTITUDE BAND			
	1	2	3	4
u_1	-.006109	-.009637	-.015505	-.020793
u_2	-.005858	-.010306	-.015392	-.018100
u_3	-.005597	-.010238	-.015364	-.018100
$\partial u_2/\partial x_1$	-.000015	-.000269	-.002197	-.006183
$\partial u_3/\partial x_1$	-.000014	-.00027	-.002198	-.006188
$\partial u_3/\partial x_2$	-.006585	-.019388	-.043538	-.064540

TABLE B-2. STANDARD DEVIATION OF GUST AND GUST GRADIENTS

SERIES TYPE	ALTITUDE BAND			
	1	2	3	4
u_1	.724352	.868642	.927039	.946672
u_2	.756057	.884176	.936133	.947373
u_3	.719277	.867329	.928437	.942133
$\partial u_2/\partial x_1$	1.139887	2.591114	4.990053	7.387333
$\partial u_3/\partial x_1$	1.670499	2.45426	4.777666	7.063241
$\partial u_3/\partial x_2$	.836263	2.225[illegible]	4.766939	7.049476

TABLE B-3. RATIO OF SQUARE ROOT OF THEORETICAL ENERGY CONTENT* TO THE OBSERVED STANDARD DEVIATION†

SERIES TYPE	ALTITUDE BAND			
	1	2	3	4
u_1	1.0134	1.0194	1.0208	1.0186
u_2	1.0048	1.0079	1.0107	1.0177
u_3	1.0050	1.0082	1.0109	1.0179
$\partial u_2/\partial x_1$	.9938	.9951	.9955	.9959
$\partial u_3/\partial x_1$	.9939	.9955	.9960	.9964
$\partial u_3/\partial x_2$	1.0039	1.0041	1.0037	1.0036

*Theoretical energy content taken from Table 2-4.

†Observed standard deviation taken from Table B-2.

TABLE B-4. MATRIX OF STATISTICAL ANAYSIS FIGURES

SERIES TYPE	ALTITUDE BAND			
	1	2	3	4
u_1	B-1	B-2	B-3	B-4
u_2	B-5	B-6	B-7	B-8
u_3	B-9	B-10	B-11	B-12
$\partial u_2/\partial x_1$	B-13	B-14	B-15	B-16
$\partial u_3/\partial x_1$	B-17	B-18	B-19	B-20
$\partial u_3/\partial x_2$	B-21	B-22	B-23	B-24

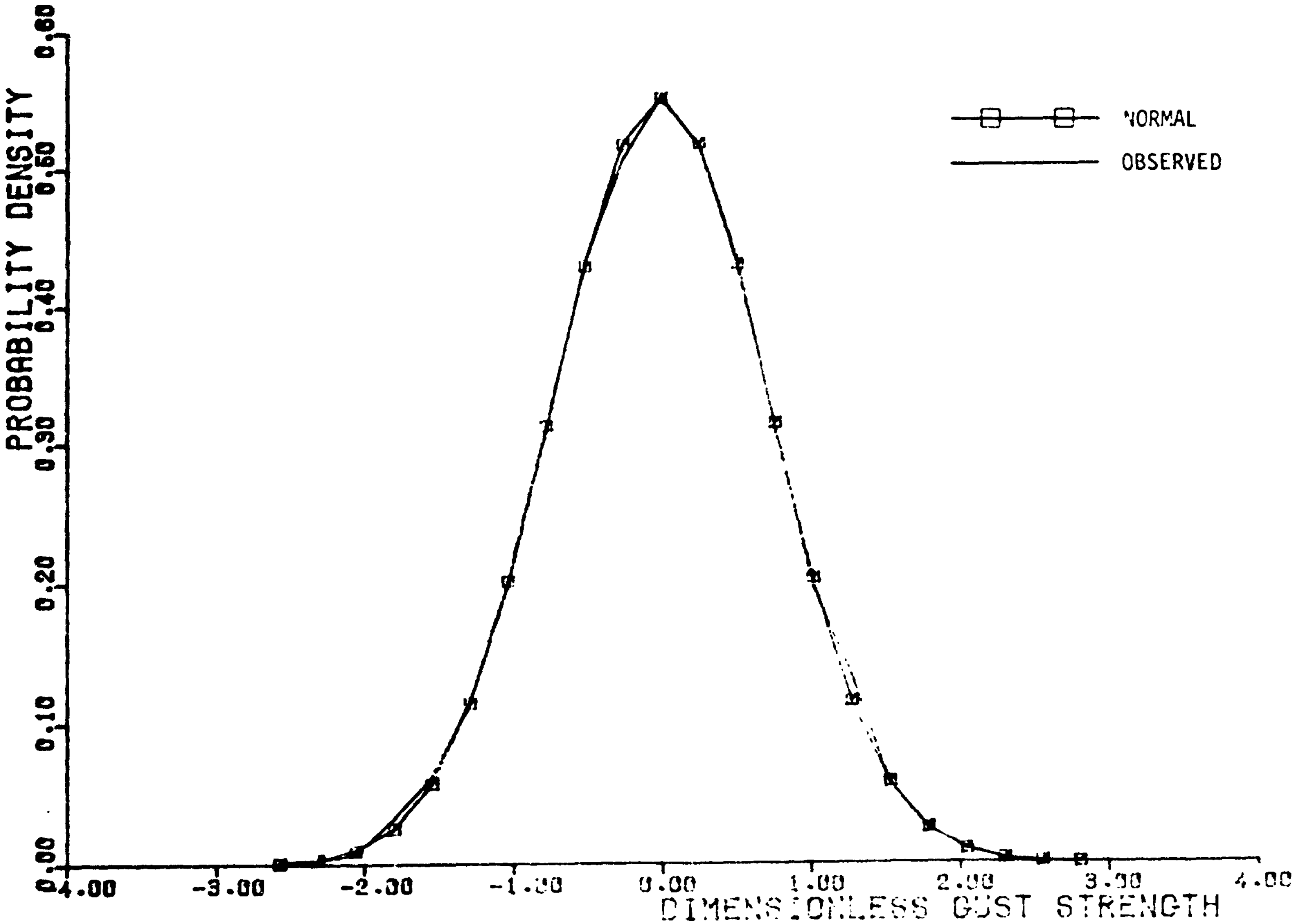

Figure B-1. u_1 - Gust Probability Density Distribution, Altitude Band #1

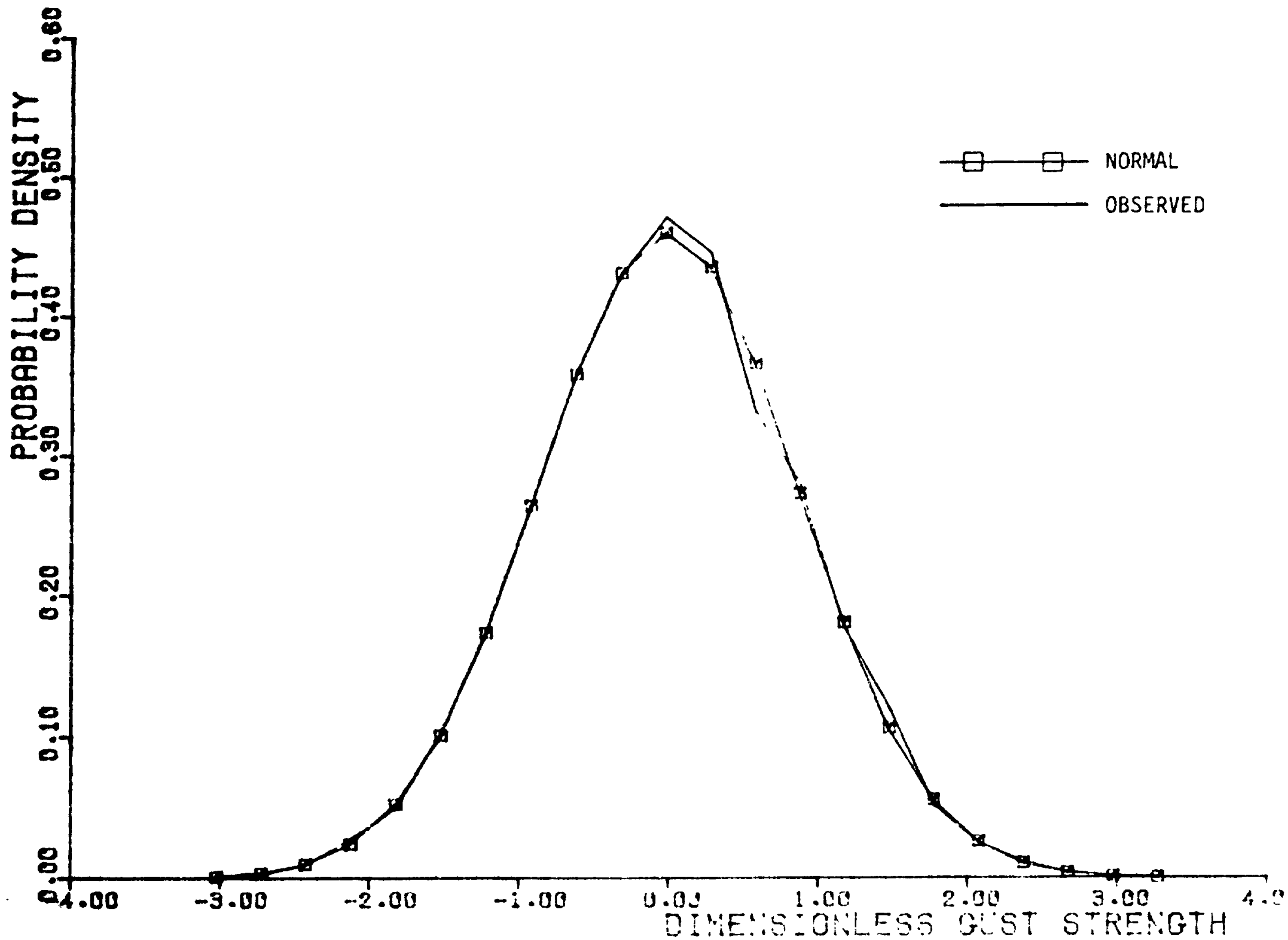

Figure B-2. u_1 - Gust Probability Density Distribution, Altitude Band #2

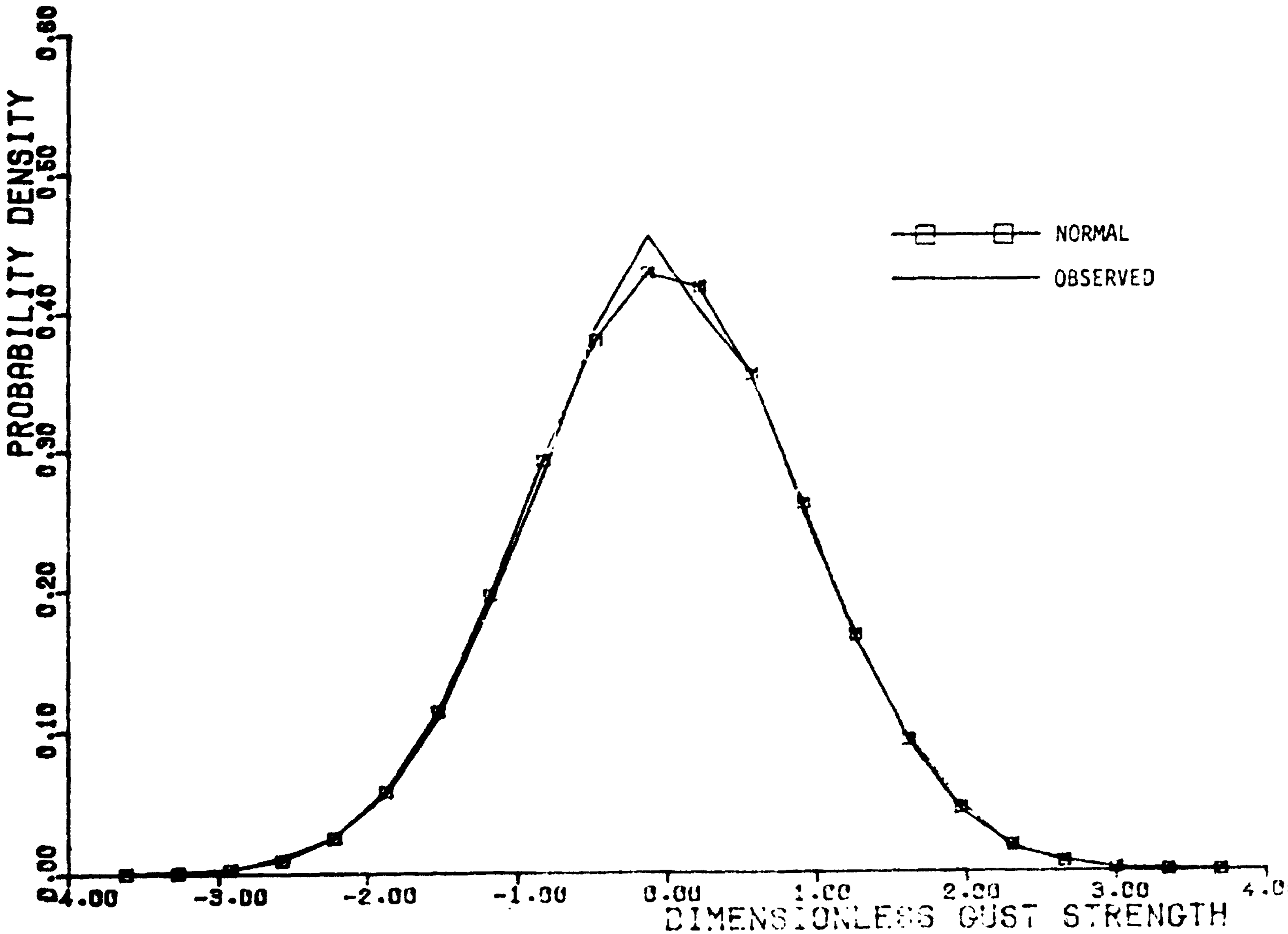

Figure B-3. u_1 - Gust Probability Density Distribution, Altitude Banc #3

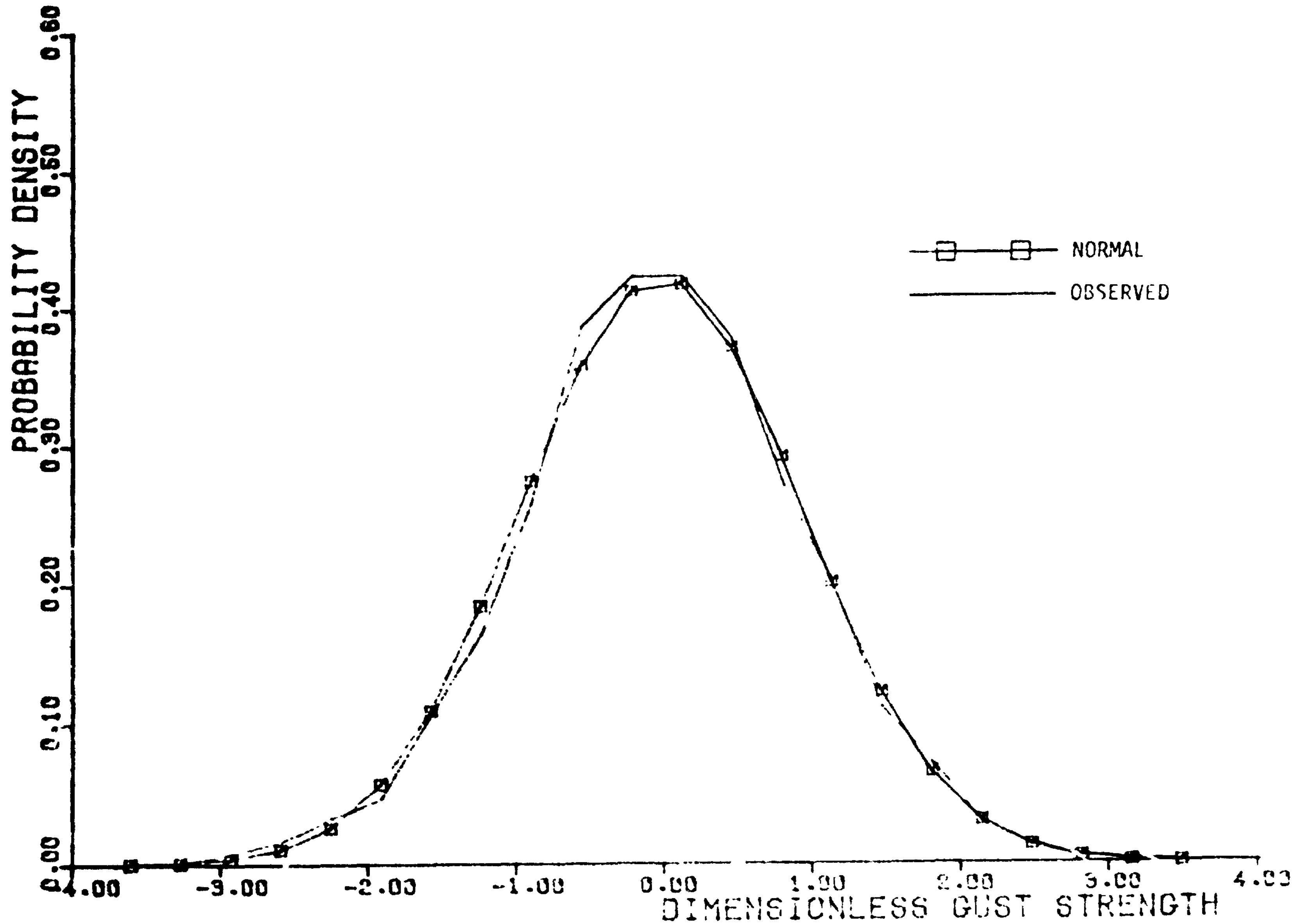

Figure B-4. u_1 - Gust Probability Density Distribution, Altitude Band #4

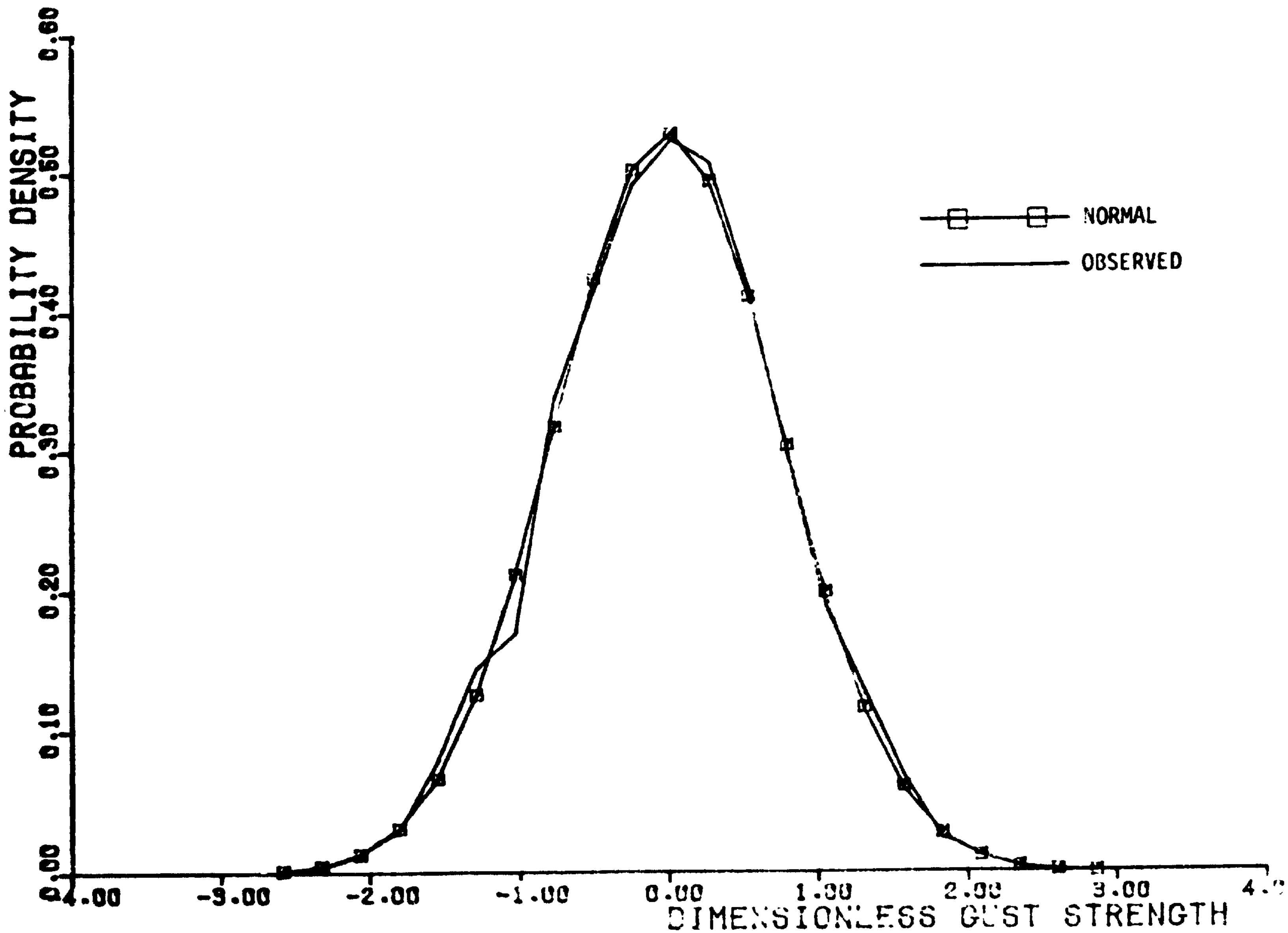

Figure B-5. u_2 - Gust Probability Density Distribution, Altitude Band #1

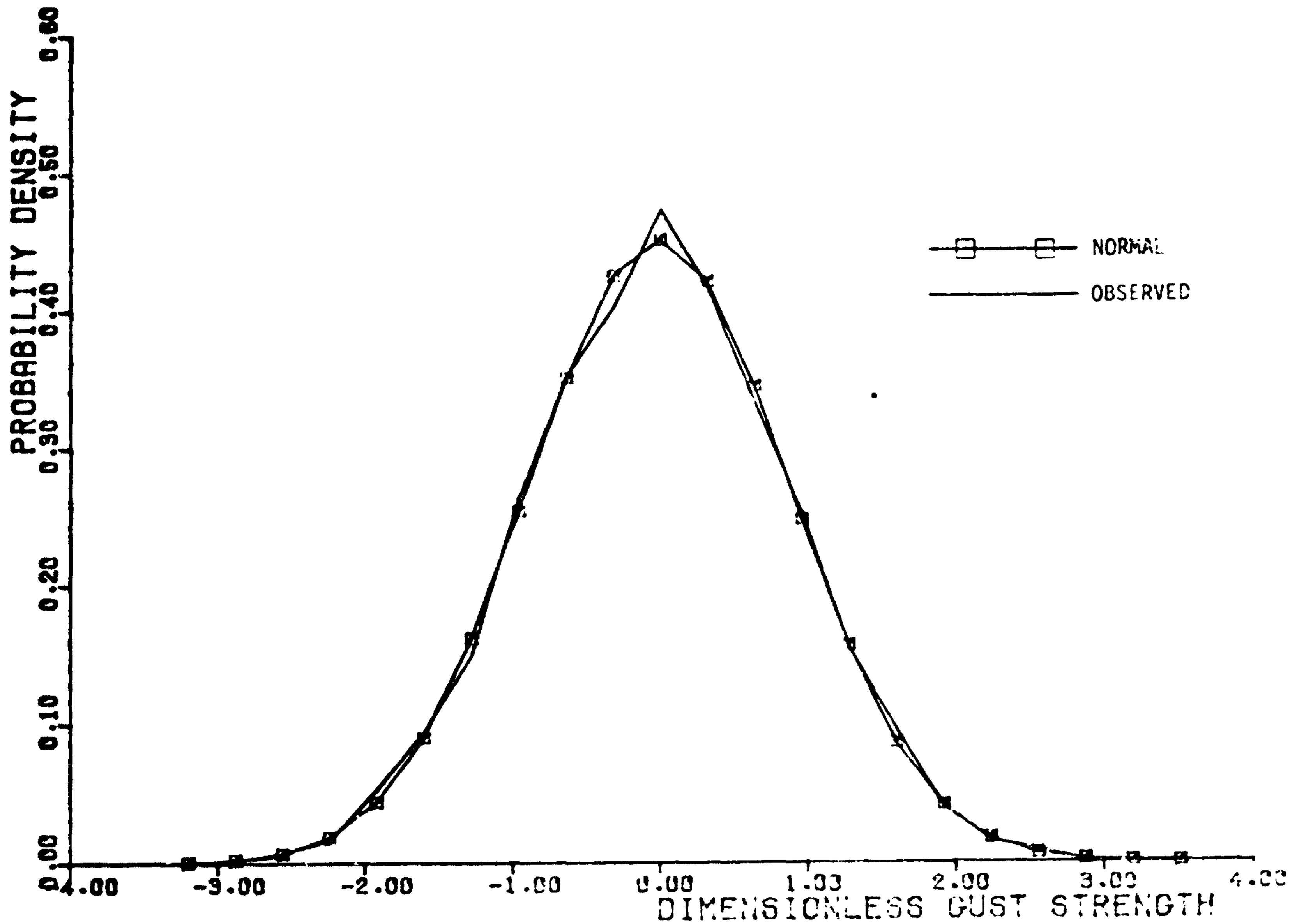

Figure B-6. u_2 - Gust Probability Density Distribution, Altitude Band #2

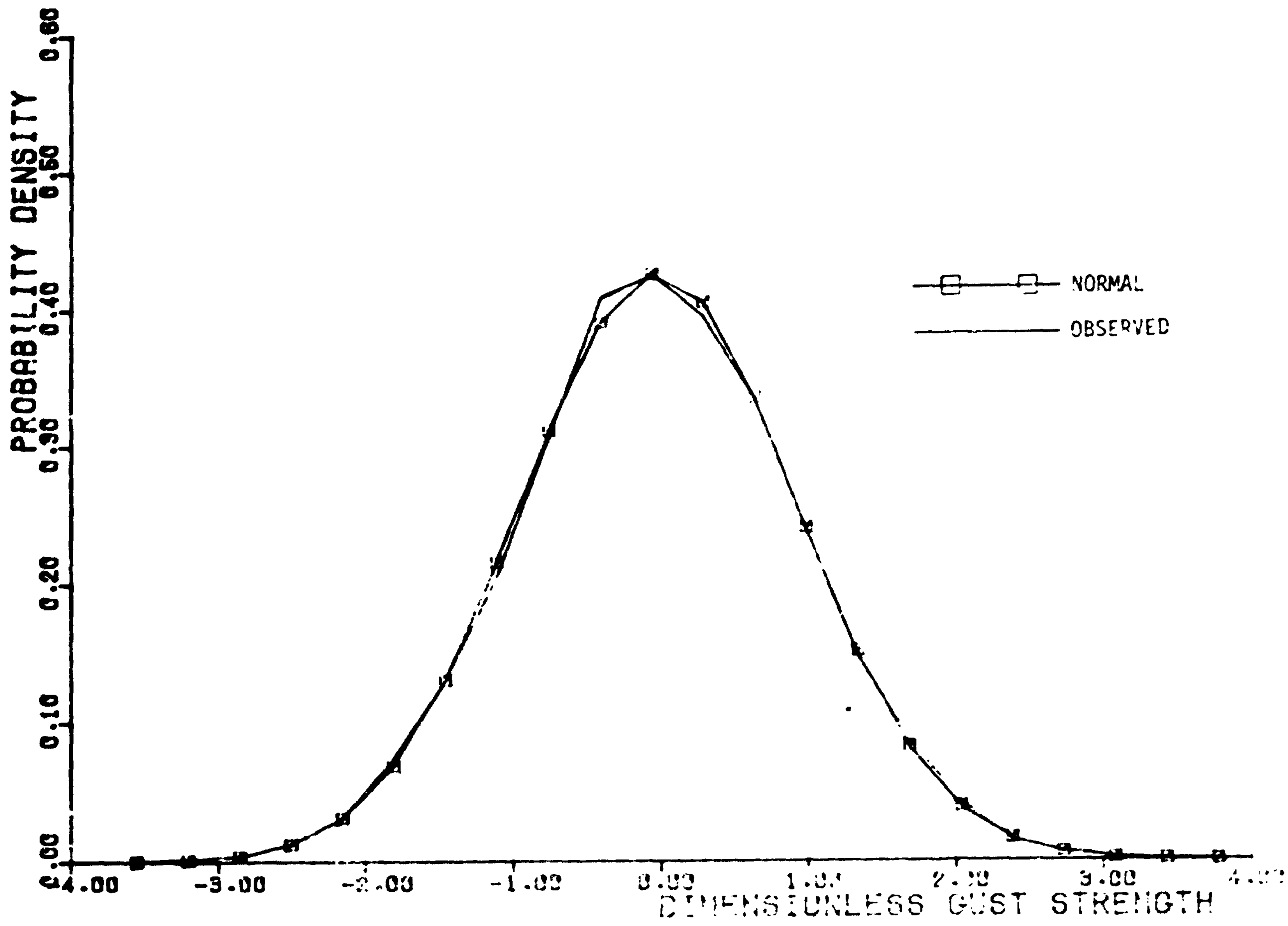

Figure B-7. u_2 - Gust Probability Density Distribution, Altitude Band #3

ORIGINAL PAGE IS
OF POOR QUALITY

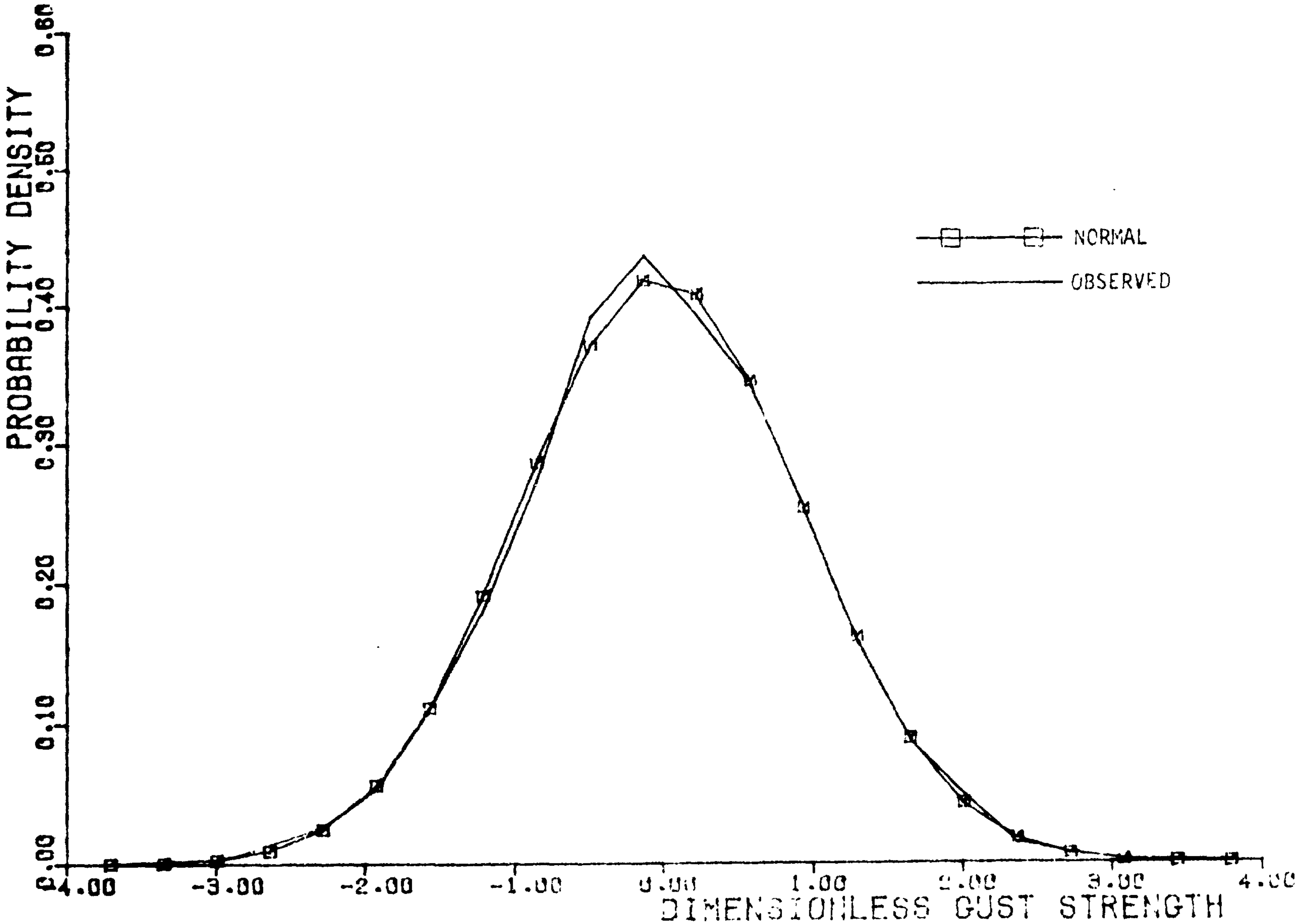

Figure B-8. u_2 - Gust Probability Density Distribution, Altitude Band #4

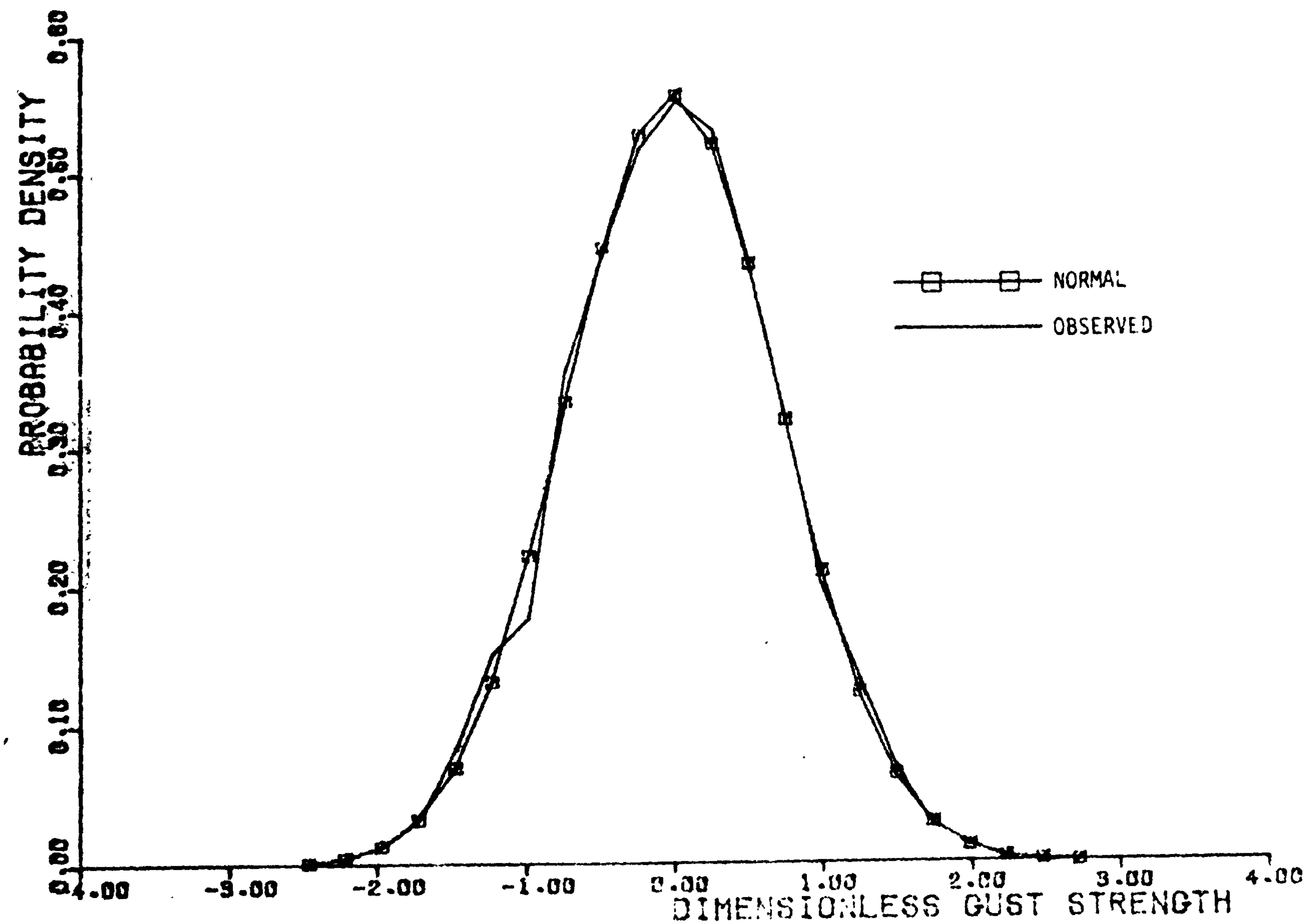

Figure B-9. u_3 - Gust Probability Density Distribution, Atmospheric Band #1

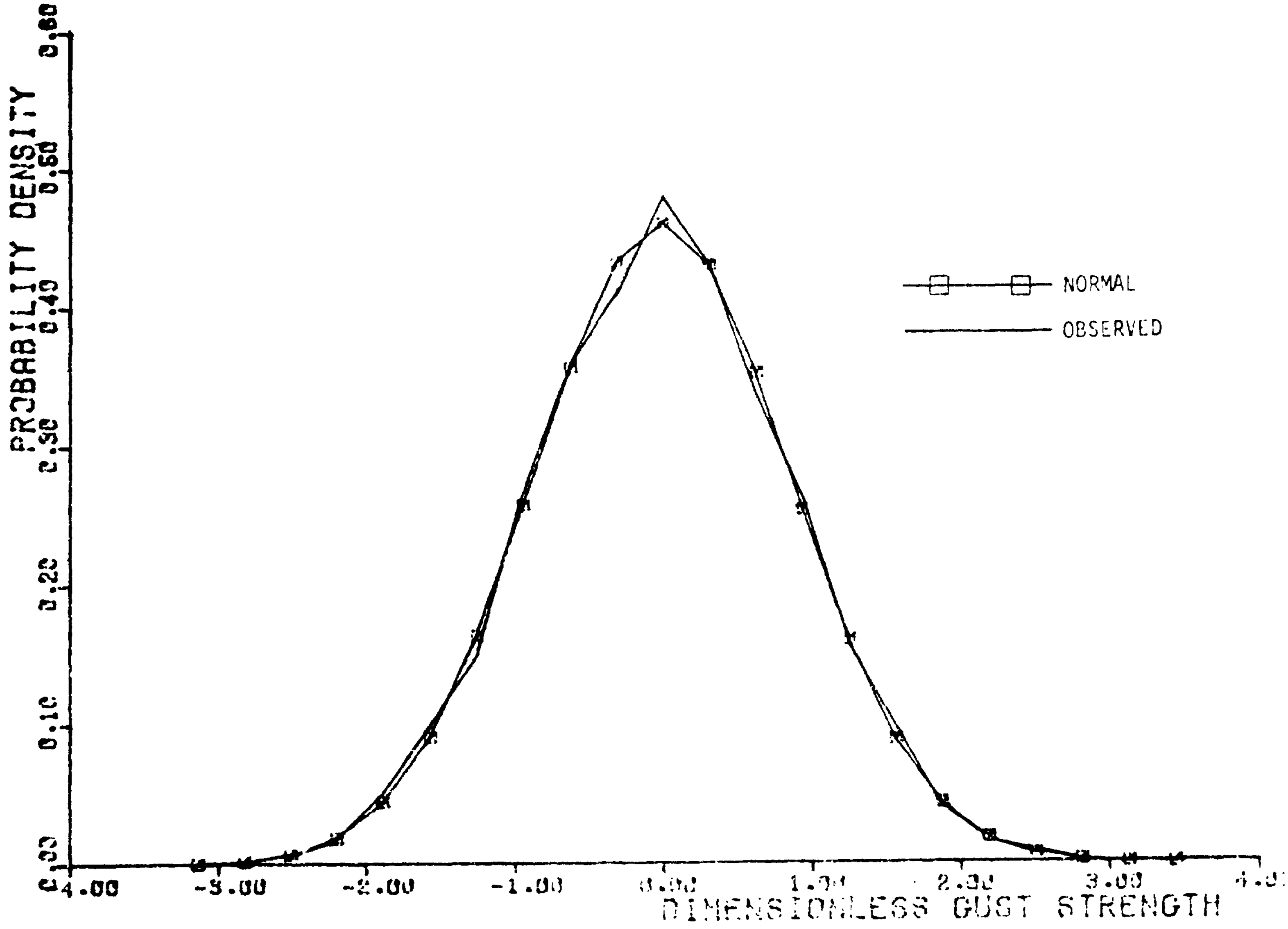

Figure B-10. u_3 - Gust Probability Density Distribution, Altitude Band #2

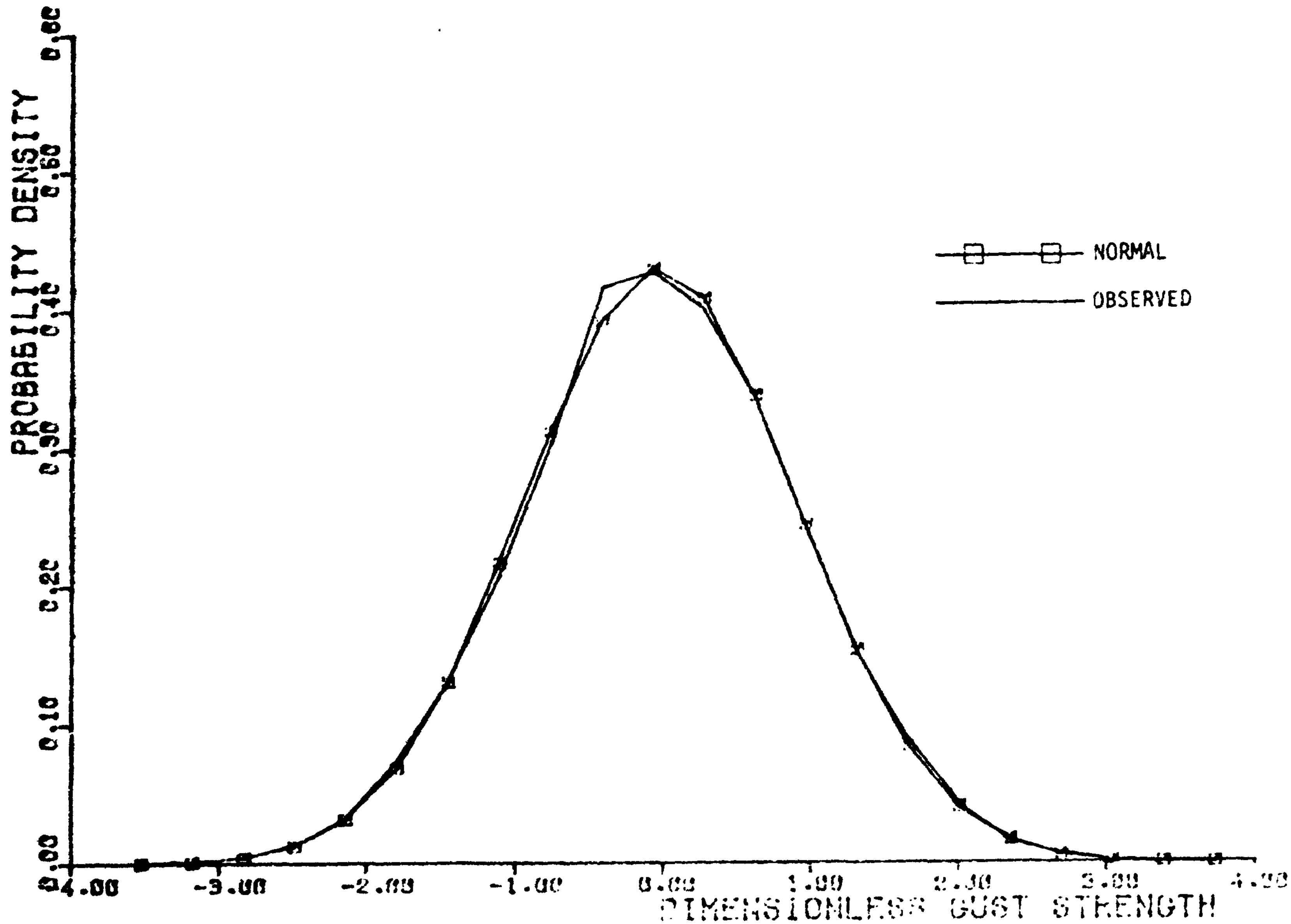

Figure B-11. u_3 - Gust Probability Density Distribution, Altitude Band #3

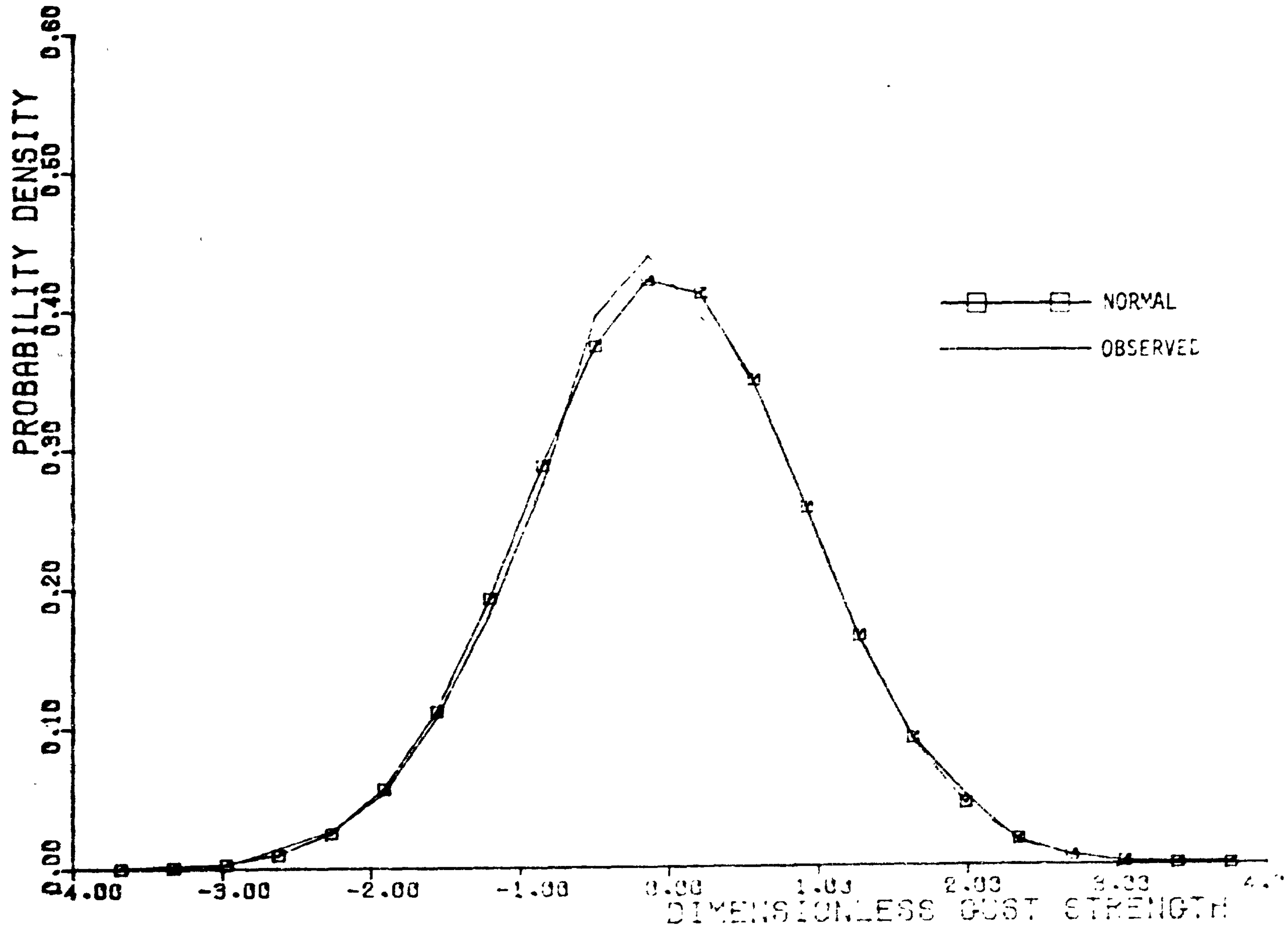

Figure B-12. u_3 - Gust Probability Density Distribution, Altitude Band #4

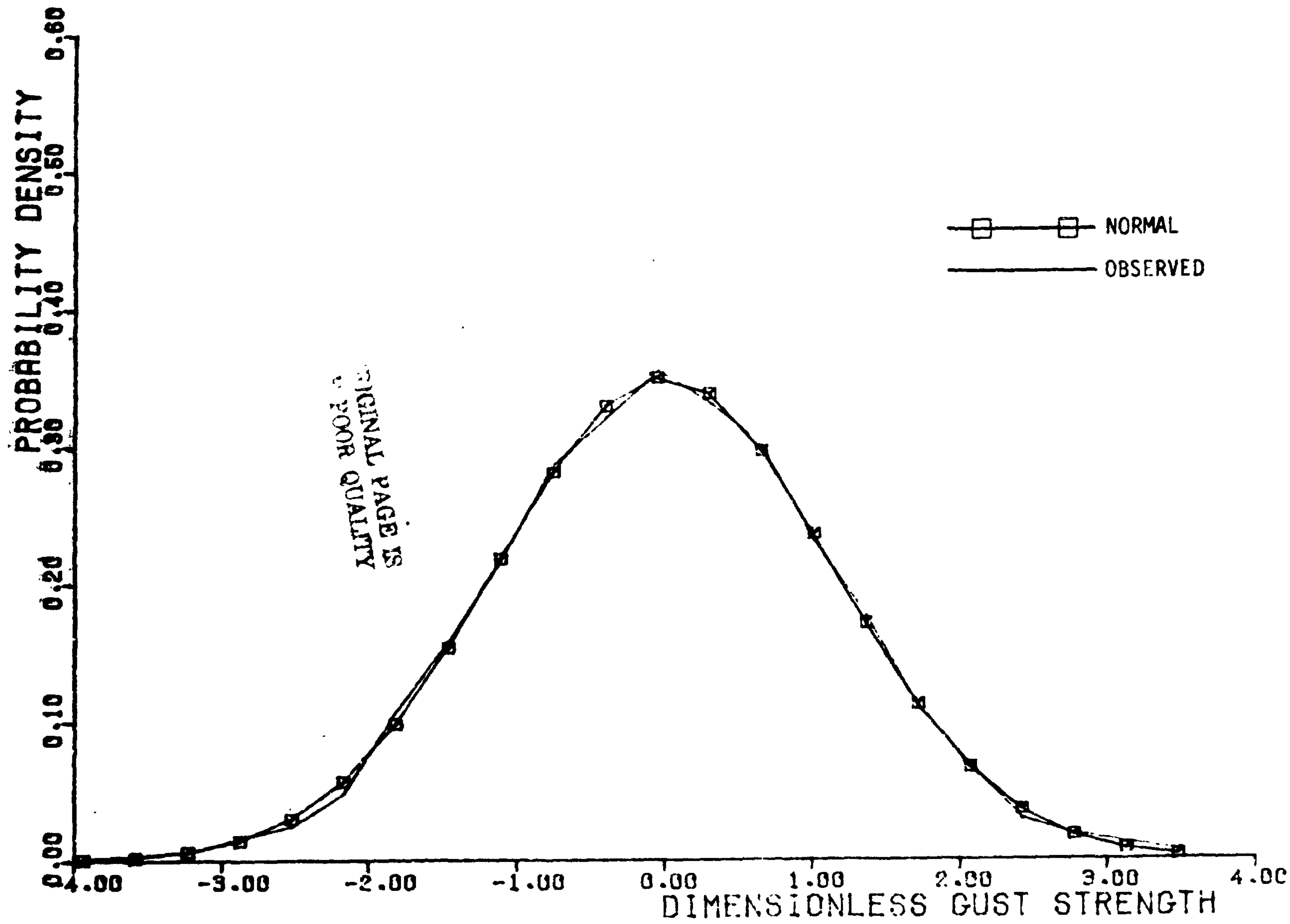

ORIGINAL PAGE IS OF POOR QUALITY

Figure B-13. $\partial u_2/\partial x_1$ - Gust Gradient Probability Density Distribution, Altitude Band #1

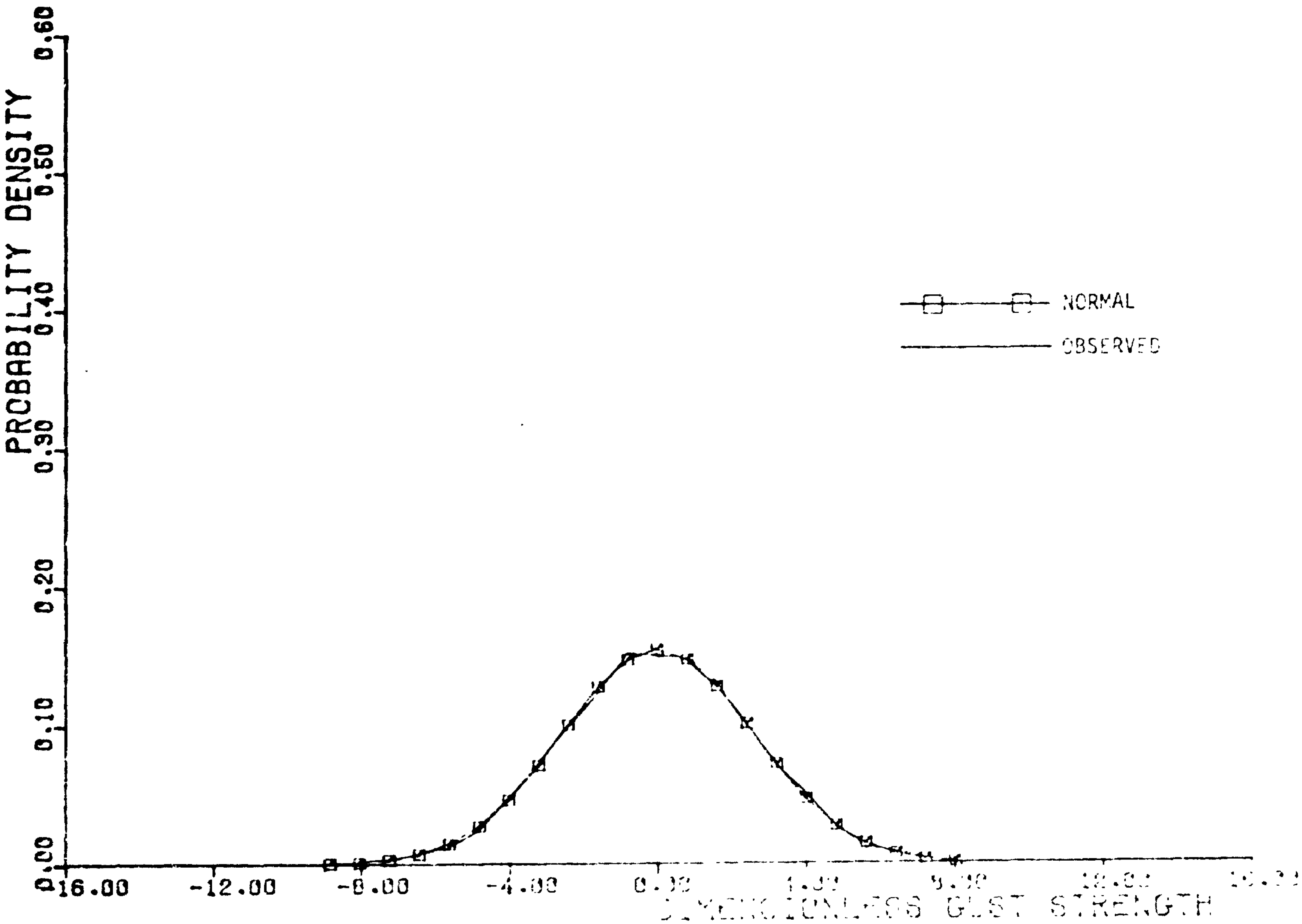

Figure B-14. $\partial u_2/\partial x_1$ - Gust Gradient Probability Density Distribution, Altitude Band #2

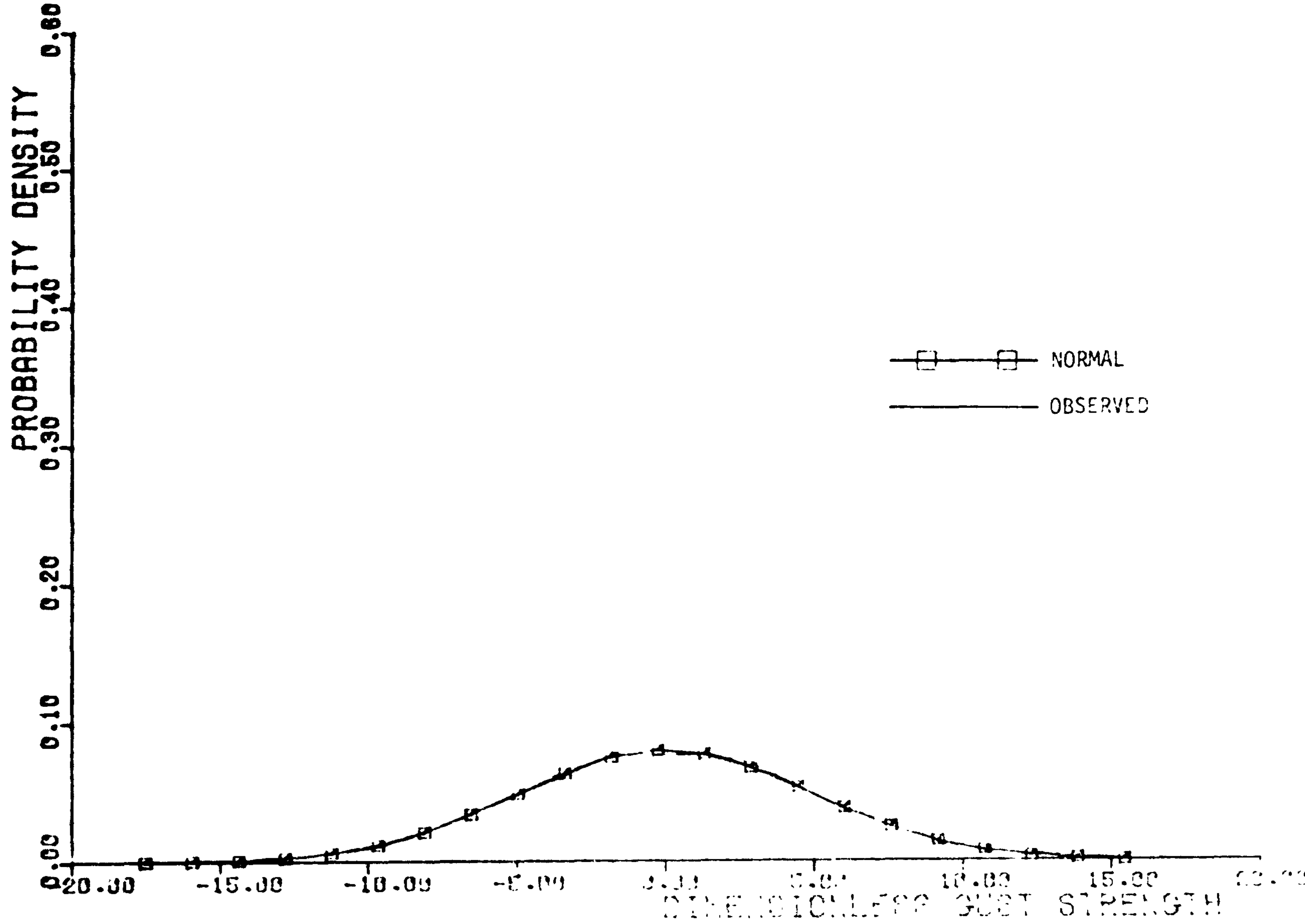

Figure B-15. $\partial u_2/\partial x_1$ - Gust Gradient Probability Density Distribution, Altitude Band #3

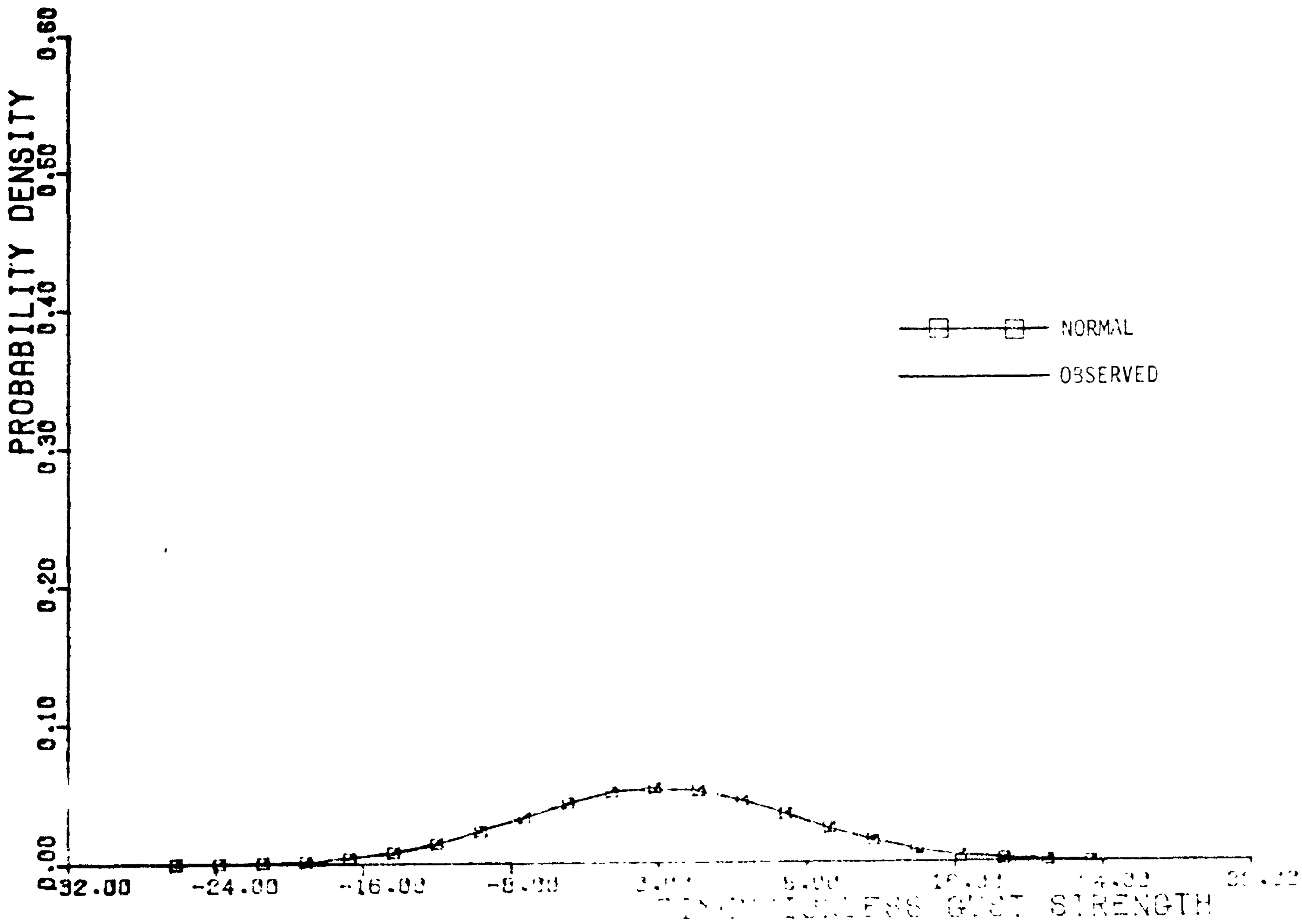

Figure B-16. $\partial u_2/\partial x_1$ - Gust Gradient Probability Density Distribution, Altitude Band #4

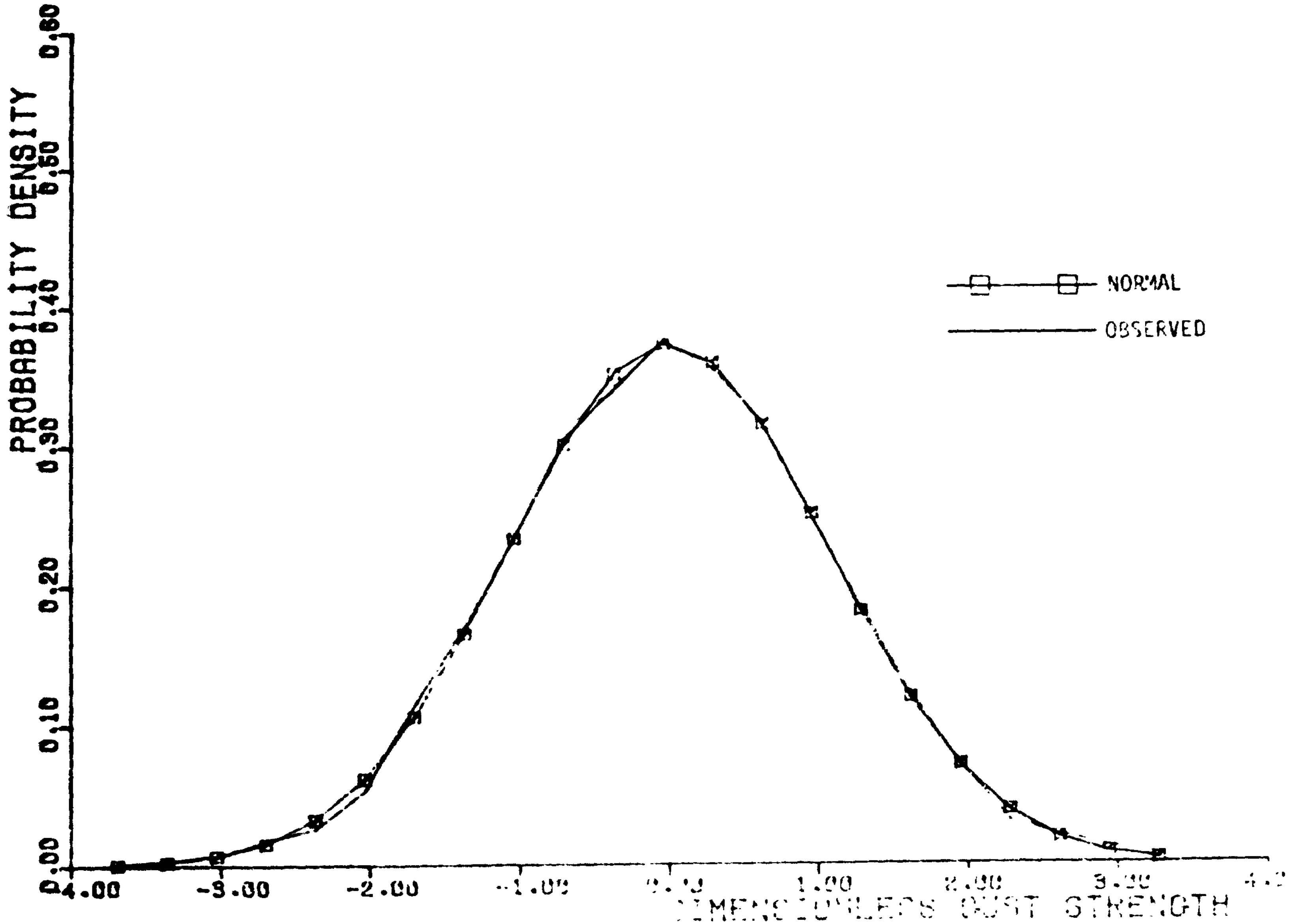

Figure B-17. $\partial u_3/\partial x_1$ - Gust Gradient Probability Density Distribution, Altitude Band #1

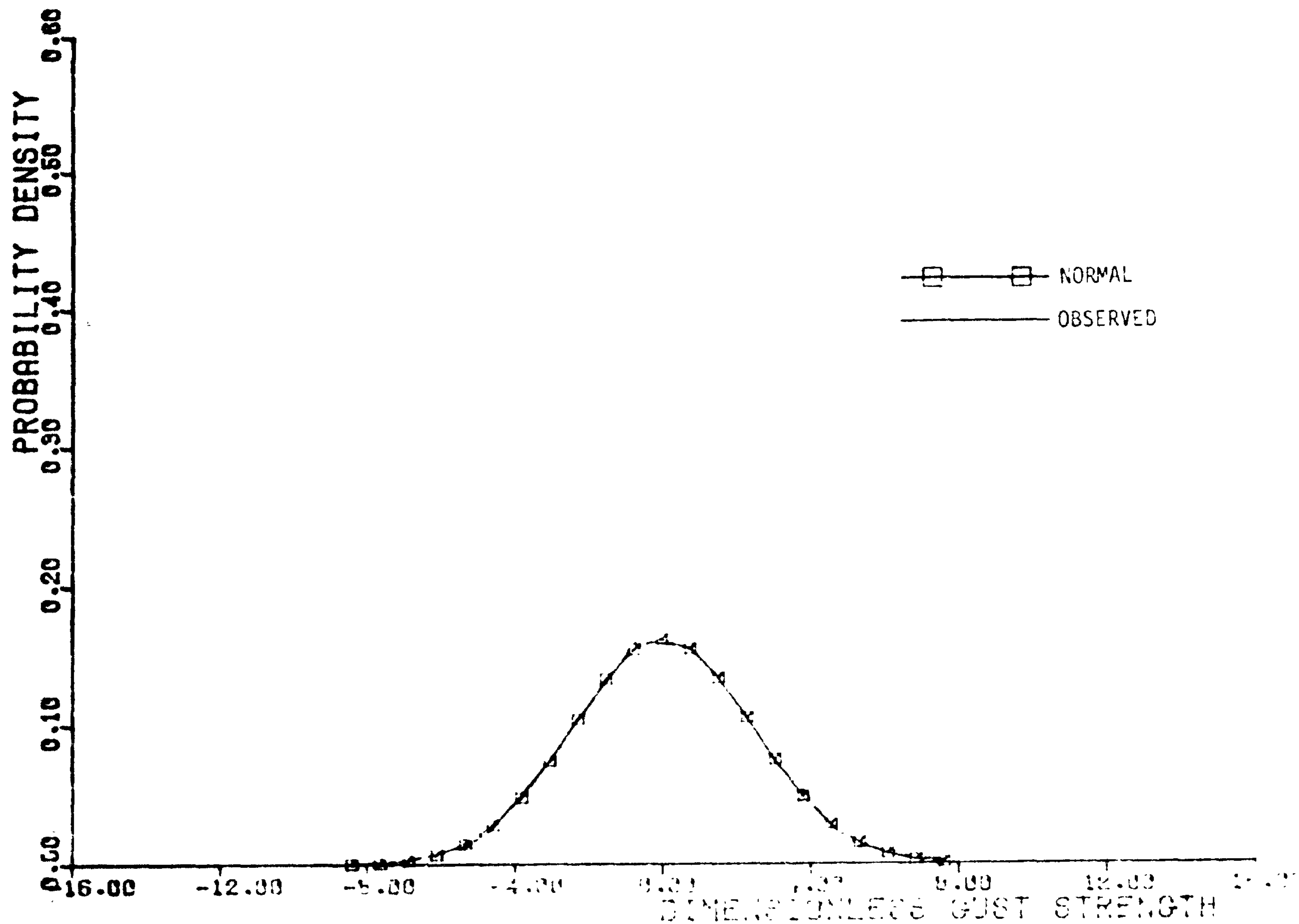

Figure B-18. $\partial u_3/\partial x_1$ - Gust Gradient Probability Density Distribution, Altitude Band #2

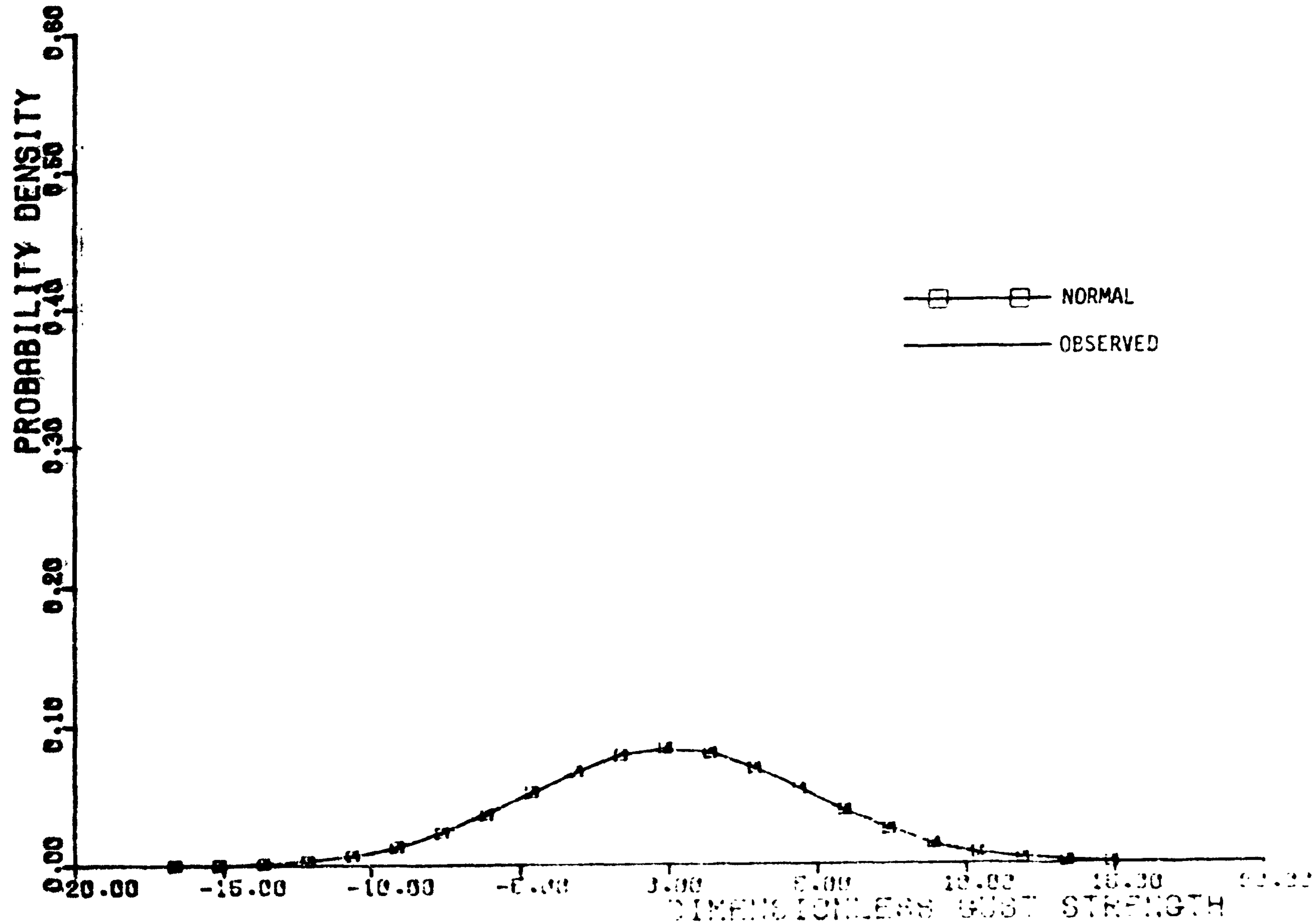

Figure B-19. $\partial u_3/\partial x_1$ - Gust Gradient Probability Density Distribution, Altitude Band #3

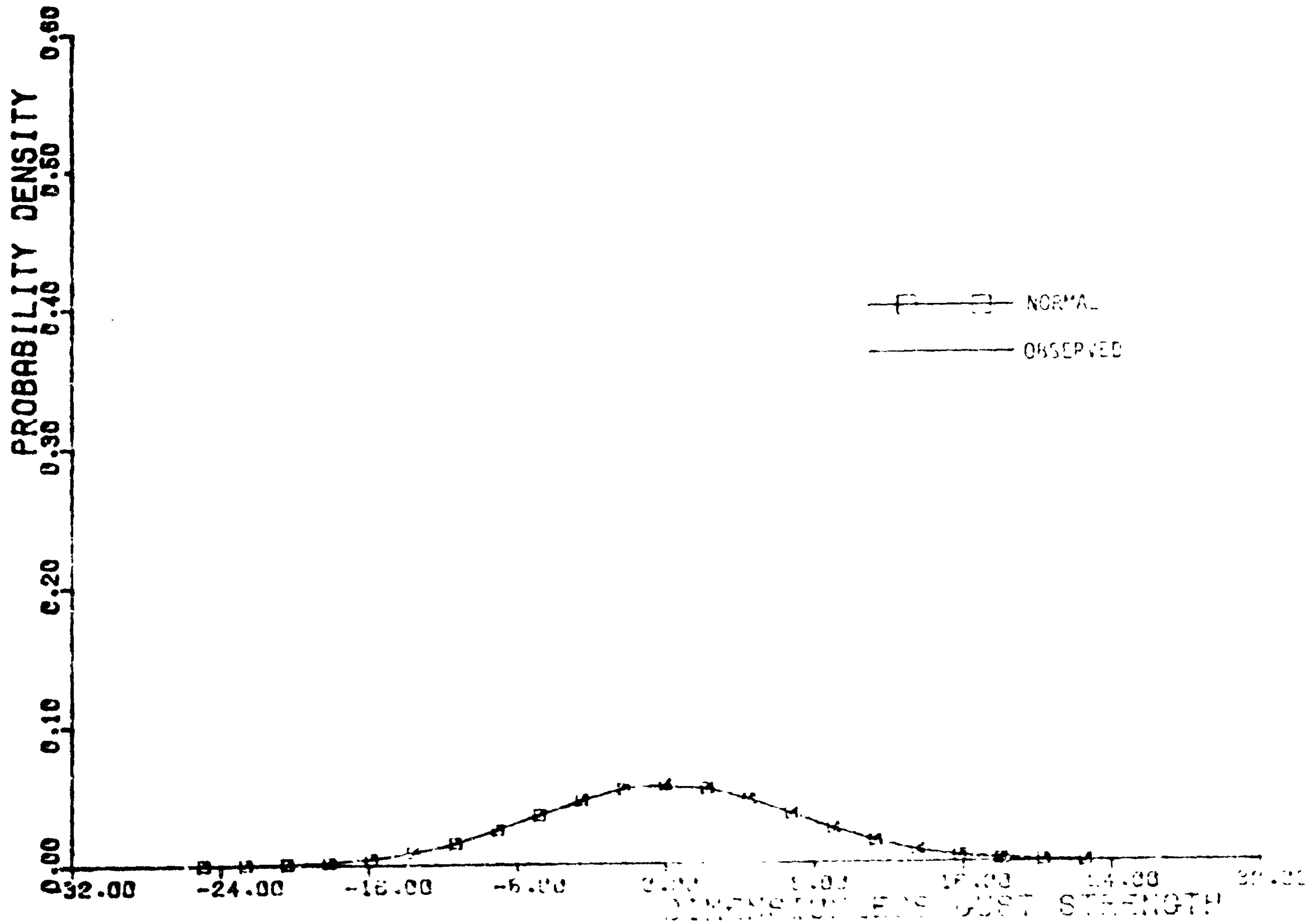

Figure B-20. u_{g_3}, x_1 - Gust Gradient Probability Density Distribution, Altitude Band #4

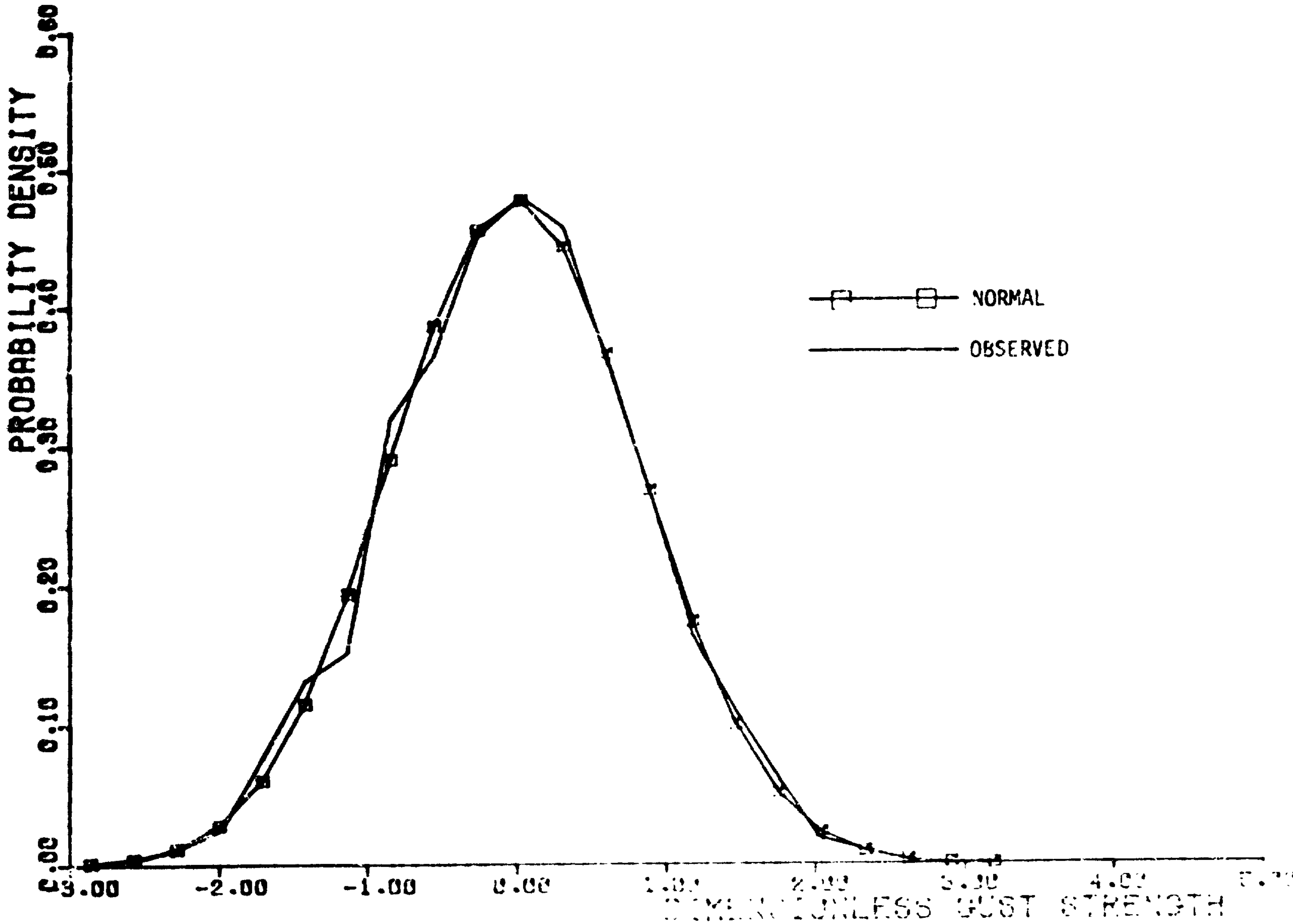

Figure B-21. $\partial u_3/\partial x_2$ - Gust Gradient Probability Density Distribution, Altitude Band #1

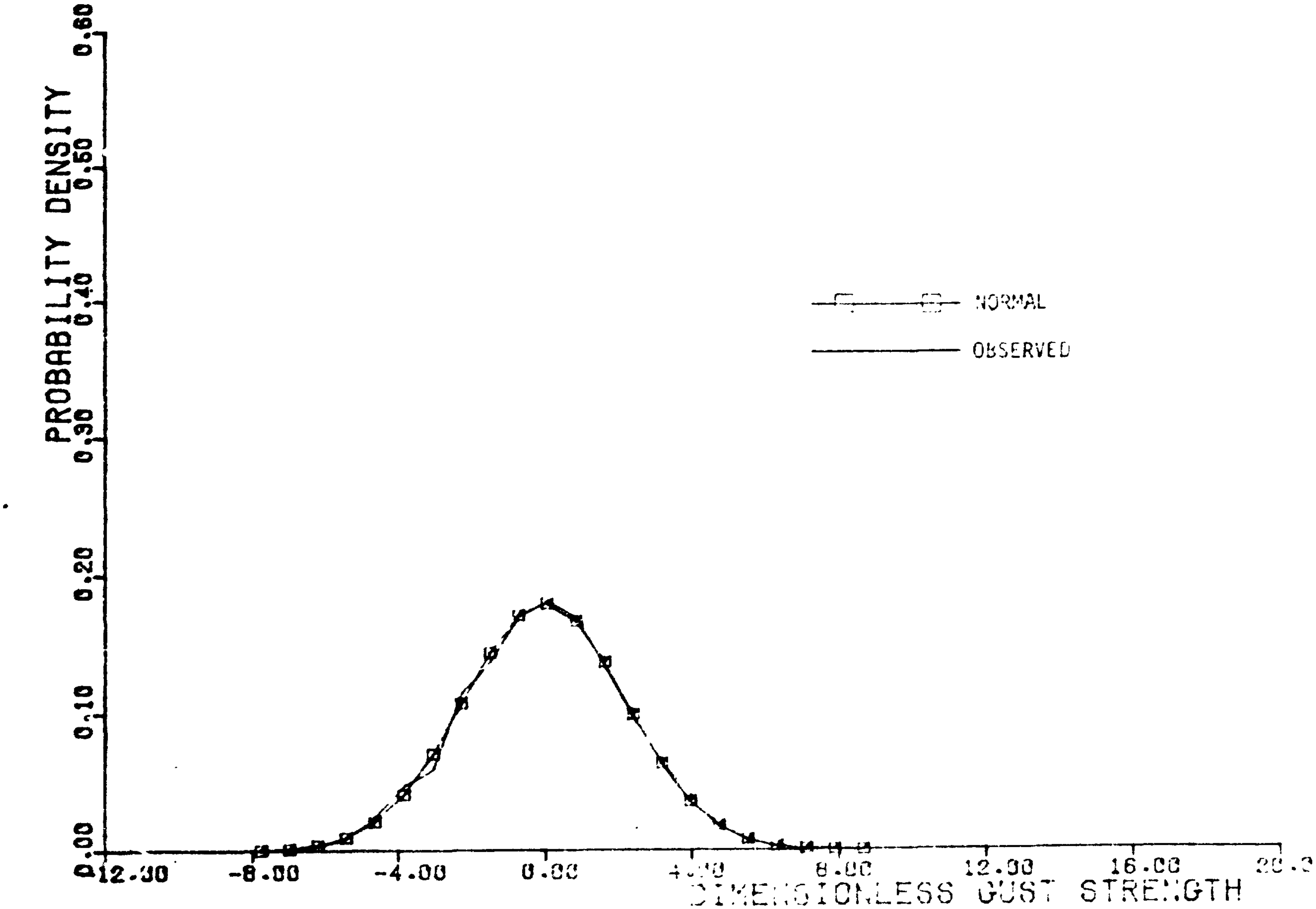

Figure B-22. $\partial u_3/\partial x_2$ - Gust Gradient Probability Density Distribution, Altitude Band #2

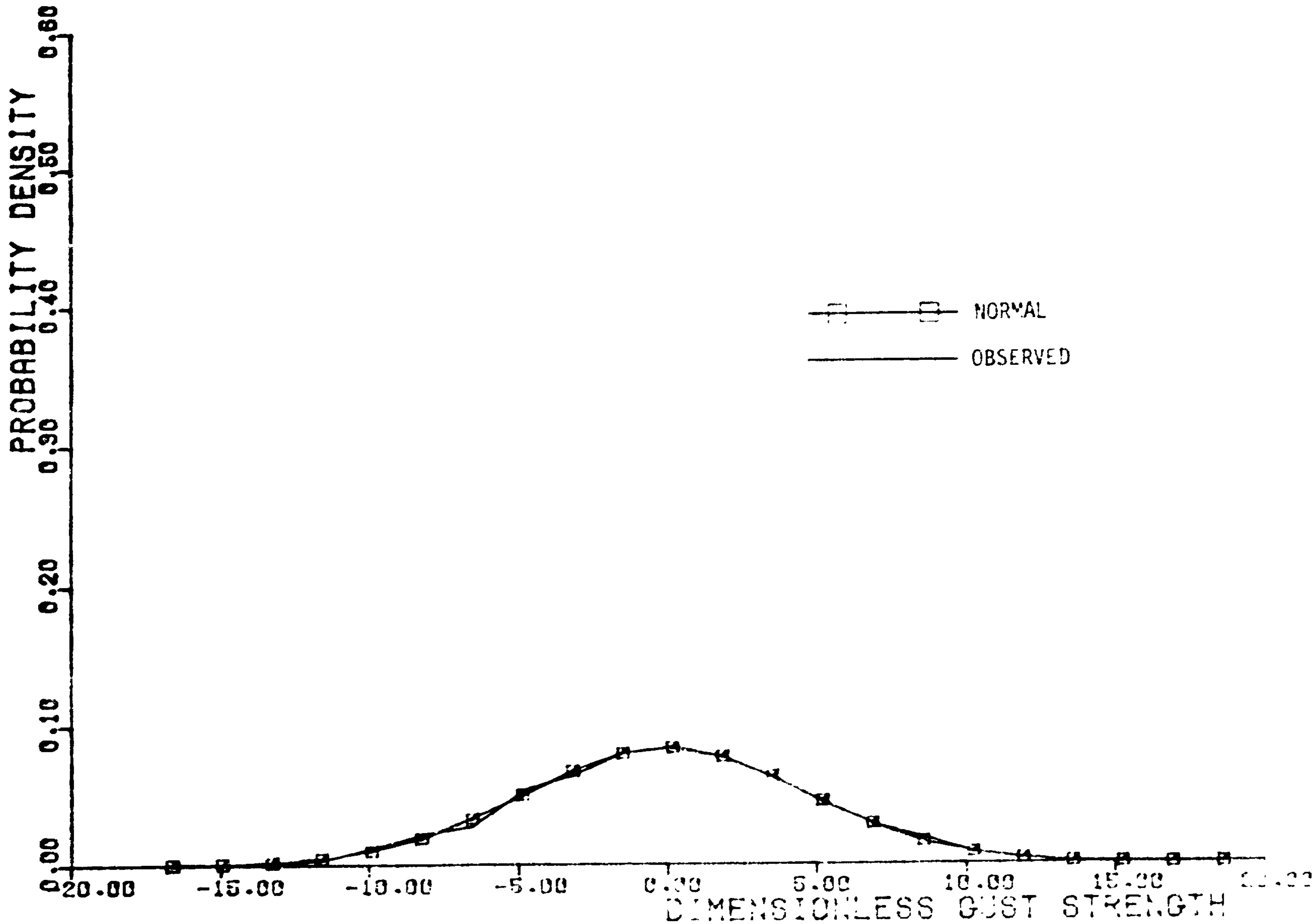

Figure B-23. $\partial u_3/\partial x_2$ - Gust Gradient Probability Density Distribution, Altitude Band #3

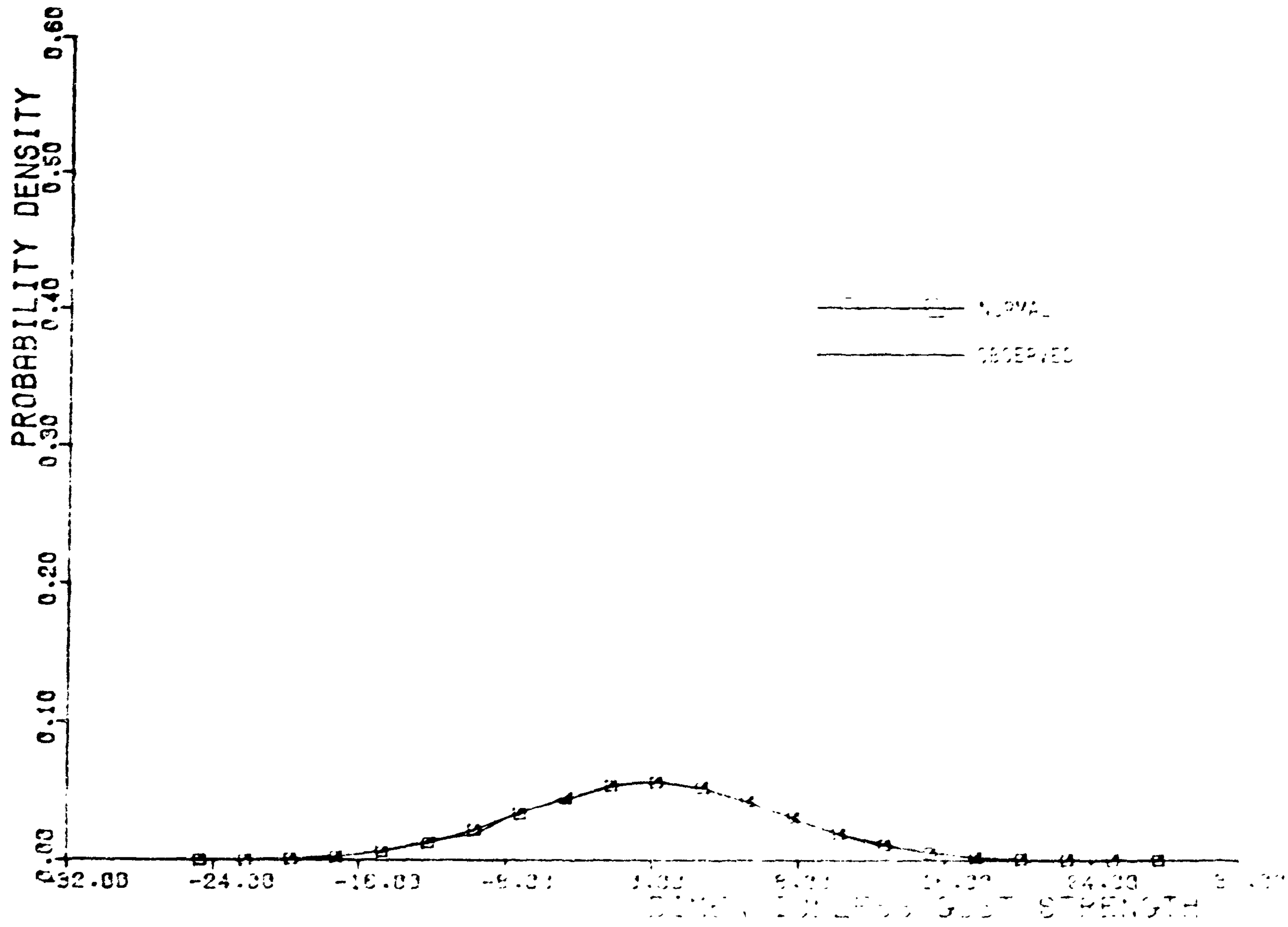
PROBABILITY DENSITY
0.00
0.10
0.20
0.30
0.40
0.50
0.60
-32.00
-24.00
-16.00
24.00
OBSERVED
STRENGTH

Figure B-24. [illegible]